Proceedings of the ASME 2012 31st International Conference on Ocean, Offshore and Arctic Engineering
OMAE2012
July 1-6, 2012, Rio de Janeiro, Brazil

OMAE2012-83561

STATE-OF-ART ON VORTEX-INDUCED MOTION: A COMPREHENSIVE SURVEY AFTER MORE THAN ONE DECADE OF EXPERIMENTAL INVESTIGATION

André L. C. Fujarra*
TPN - Numerical Offshore Tank
University of São Paulo, Brazil
(afujarra@usp.br)

Guilherme F. Rosetti
TPN - Numerical Offshore Tank
University of São Paulo, Brazil
(guilherme.feitosa@tpn.usp.br)

Jaap de Wilde
MARIN - Maritime Research Institute Netherlands
Wageningen, the Netherlands
(j.dewilde@marin.nl)

Rodolfo T. Gonçalves
TPN - Numerical Offshore Tank
University of São Paulo, Brazil
(rodolfo_tg@tpn.usp.br)

ABSTRACT

After one decade of experimental investigation, the Vortex-Induced Motion – VIM phenomenon deserves a comprehensive survey concerning the advances related to its understanding, mainly under the consideration of the fundamental aspects that keep it in a close relationship to the dynamic behavior of the same phenomenon acting on slender bodies, the well known Vortex-Induced Vibration – VIV. A considerable amount of results can be found in the literature, although there are few works dealing with a general view of the problem. Probably, the main reason for such a large amount of works with no interaction between themselves and, consequently, without a common understanding about VIM might be due to its technological origin, featured by huge platforms with a variety of geometrical details, which ends up placing the researches more on the field of the faithful reproduction of the features in small-scale and less on the global understanding of the phenomenology regardless the floating system, e.g. a spar platform, a monocolumn or even a semi-submersible or a tension-leg platform. Obviously, no one should disagree that there is part of the research that must keep a faithful relationship with the full scale, however, in most of them it is possible to identify the common fundamentals concerning the fluid-structural interaction. The aim of the present work is to address a comprehensive evaluation of the experimental investigations during the past decade on the VIM, trying to gather a general understanding about its phenomenology including some comparisons to VIV. As a result, some relevant aspects are pointed out for a more prospective way of research.

Keywords: VIM, vortex-induced motion, comprehensive survey, experiments.

GENESIS OF VIM ON LARGE FLOATING UNITS

According to Kokkinis et al. [36], since the Genesis spar platform started working in Gulf of Mexico in 1997, several occurrences of VIM were observed, always complying with the predictions based on small-scale experiments carried out in late 1995, which took into account a spar outfitted with helical strakes of 10% of the hull diameter in height, as well as the potential presence of 100-year loop/eddy current. Despite those concerns, in 2001 VIM response amplitudes of more than twice the predicted values during the project design phase were observed as a result of a millennium eddy current reaching the Genesis location. As a consequence, a wide range of investigation started being conducted not only concerning the VIM phenomenon act-

*Presently at MARIN as visiting researcher ing on spar platforms such as Genesis, but also comprising to its potential occurrence on monocolumn, semi-submersible and tension-leg platforms.

After a phenomenological background presented as follow, the next sections summarize a comprehensive survey on this issue, gathering most of the experimental results available and reported in the open literature during more than one decade of investigation. Moreover, important concerns on the experimental approach for the state-of-art in R&D are presented, which are based not only on the literature results, but also on the experience that has been gathered by the authors.

PHENOMENOLOGICAL BACKGROUND

Fundamental aspects

Essentially speaking, VIM and VIV are the same phenomenon, presenting as a resonant behavior due to fluid-structure interaction. In both cases, as a result of the balance between the energy provided by the fluid flow and the energy dissipated by damping acting on the system (a slender cylinder or even a floating unit), a *self-limited* oscillation of amplitude close to the dimension of cross section is triggered by the frequency of vortex shedding, approximately equal to one of the natural frequencies involved. It is well known that the frequency of shedding is linearly dependent on the ratio between flow velocity and dimension of cross section, see eq. (1), where *St* is the Strouhal number, an inherent feature of the cross section, practically invariant for a large range of Reynolds number, *Re*. In fact, both parameters play an important role in this fluid dynamic mechanism, justifying the details presented further on.

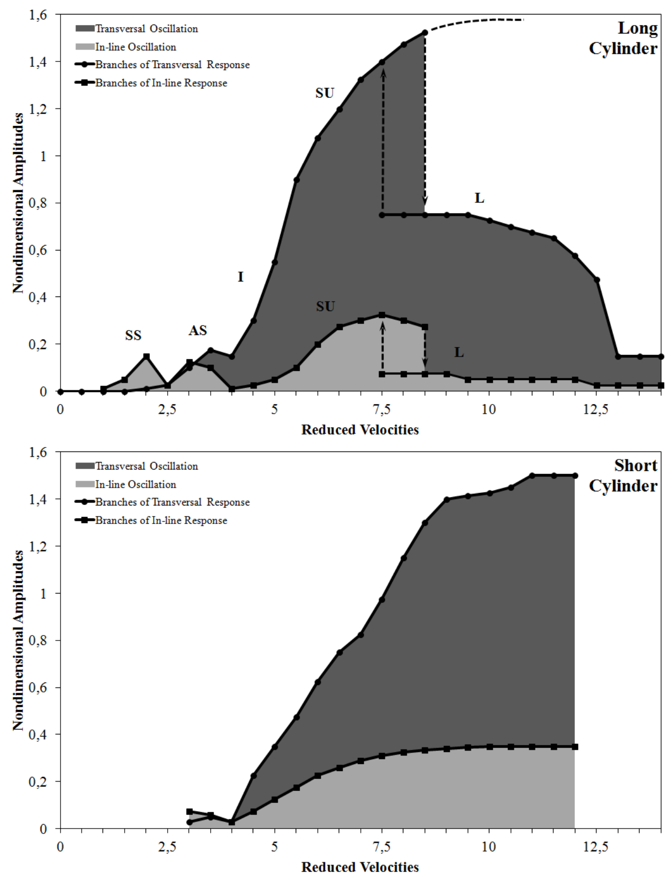

FIGURE 1: Qualitative comparison between nondimensional amplitudes as function of the reduced velocity.

$$f_s = St \cdot \frac{U}{D}, \qquad (1)$$

The *self-excited* behavior featured by the synchronization between the frequency of shedding and a natural frequency of the system is kept for a considerable range of flow velocities, inside which the transverse and in-line amplitudes of oscillation can display several branches of response, mutually related as shown in Fig. 1 and Tab. 1, the latter presenting the respective details about the relation between response frequencies (f_y transverse and f_x in-line) and frequency of shedding, f_s.

From Fig. 1 it can be observed that VIV and VIM can induce response amplitudes up to 1.5 times the cross section main dimension of the cylinder, irrespective if it is long or short, but in both cases as a result of a notable coupling with the in-line oscillations. Moreover, for both cases (long and short cylinders), the transverse amplitude starts increasing at reduced velocity of approximately 4, as a consequence of the synchronization, *i.e.* $f_y \approx f_n \approx f_s$, see comparisons in Tab. 1. Although two behaviors of in-line resonance can be noticeable for reduced velocity below 4, it is after this value that the oscillations in this direction become really important. Although the in-line amplitudes of circa 0.35 are not so large, they contribute for larger amplitudes in the transverse direction. In fact, in-line oscillations of this order are responsible for an important difference for some cases of VIM, being the absence of a *Lower branch (L-branch)* of transverse amplitudes as it is verified for long cylinders in the case of reduced velocities larger than approximately 8. As it will be discussed, this behavior has close relation to the ratio between the structural mass and the fluid mass displaced by the system.

Because of its low frequencies, as well as its nature is in some aspects different from that observed for the VIV on slender bodies, such as the one concerning the maintenance of in-line oscillations, VIM was considered a distinct phenomenon, especially in the first years of research. Nowadays, in consequence of intensive investigation, it is well known that VIM is a particular case of VIV. VIM and VIM share the same mechanism of fluid-structure interaction, *i.e.* the same *self-excited* and *self-*

limited behavior. However, the designation VIM is used for large floating offshore structures, mainly due to the larger oscillation periods of more than 10 seconds.

TABLE 1: Qualitative behavior for the response frequencies (f_y transverse and f_x in-line).

LONG CYLINDER

V_r	Transverse Motion	In-line Motion
< 1.0	no VIV	no VIV
1.0 to 2.5	$f_y \cong 0$	$f_x = f_n = 2f_s$
2.5 to 4.0	$f_y = f_n/2 = f_s$	$f_x = f_n = 2f_s$
4.0 to 5.0	$f_y \approx f_n \approx f_s$	$f_x \approx 2f_n \approx 2f_s$
5.0 to 12.5	$0.8f_n \leqslant f_y \leqslant 1.1f_n$, $f_s \approx f_n$	$f_x \approx 2f_n \approx 2f_s$
> 12.5	no VIV	no VIV

SHORT CYLINDER

V_r	Transverse Motion	In-line Motion
2.5 to 4.0	$f_y \approx f_n/2$	$f_x \approx 2f_y$
4.0 to 5.0	$f_y \approx f_n$	$f_y \leqslant f_x \leqslant 1.2f_y$
5.0 to 7.0	$f_n \geqslant f_y \geqslant 0.75f_n$	$1.2f_y \leqslant f_x \leqslant 2f_y$
> 7.0	$0.75f_n < f_y \leqslant 1.1f_n$	$f_x \approx 2f_y$

Main parameters and aspects for VIM phenomenon

In spite of the mentioned similarities between VIM and VIV, part of the phenomenology concerning VIM on floating units deserves particular attention, mainly in terms of four decisive aspects for its dynamic behavior. According to Fig. 2, VIM is really a particular case of the VIV phenomenon, but dynamically featured by the higher Reynolds numbers, oscillation in more than one degrees-of-freedom, the intrinsic characteristics of low aspect ratio (particularly defined for each case of floating unit) and by very small mass ratio (for some platforms even lower than unity).

It is important to emphasize that, taking into account the poor investigation about the effects of some parameters and aspects in terms of floating units, the discussion herein presented was partially based on results from bare cylinders. This will not bring any misunderstanding for the aims of this review, but rather will possibly allow a more wide meaning for the observed phenomenology by means of testing at small-scale.

Reynolds number The Reynolds number is a nondimensional parameter representing the ratio between inertia and friction fluid forces involved in separated flows, eq. (2). For monocolumn platforms, for example, it can be easily greater than $1.0 \cdot 10^7$, definitely in the supercritical region.

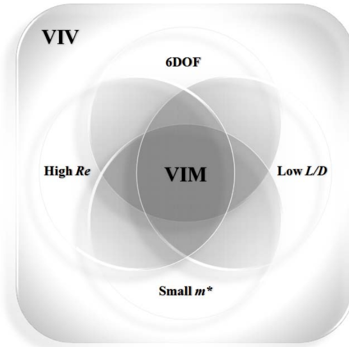

FIGURE 2: VIM is a particular case of VIV on cylinders with low aspect ratio, small mass ratio, at least 2DOF and high Reynolds numbers.

$$Re = U \cdot D/\nu \tag{2}$$

Although it is the most important parameter to be considered when seeking for similarity between hydrodynamic behaviors, in the case of small-scale tests with floating units subjected to the VIM phenomenon, it becomes an infeasible task since the typical scale factor applied varies from $\lambda = 40$ to 100 due to the restrictions imposed by the available facilities. For instance, a monocolumn of $100m$ in diameter operating in a current of approximately $1m/s$, even applying a scale of $\lambda = 100$, should be tested at velocities of $100m/s$, which is impractical for any laboratory. Furthermore, another nondimensional parameter must be kept similar to full scale during the small-scale tests, namely the Froude number $Fr = U/\sqrt{g \cdot D}$, which is mandatory to avoid unreal effects of wave generation at the free surface.

As discussed in van Dijk et al. [60], the alternative procedure for reliable model tests of floating units is based on the Froude scaling, resulting in Reynolds numbers according to $Re^{model} = Re^{full}/\sqrt{\lambda^3}$. It is well known that drag force of a circular cylinder varies substantially from the subcritical to supercritical region, as a result of boundary layers changing from laminar to turbulent. This could be a problem for the model tests of floating units, but considering that such a behavior is much less pronounced as the surface roughness increases (defined by the ratio between the mean height of the surface protrusions and dimension of the cross section, k/D), sufficient roughness is added to the model surface in order to emulate a supercritical regime during tests with Reynolds numbers below the critical value, therefore avoiding substantial change in the flow regime and consequently on the drag force. The increase of surface roughness is also important to minimize inherent effects coming from the scaling.

Although based on a straightforward and plausible procedure, the comparison between VIM motion coming from subcritical and supercritical regimes deserves much more attention, especially due to some additional aspects related to the response amplitude dependence on the Reynolds number and surface roughness. According to Blevins and Coughran [2], experiments on VIV of bare cylinders elastically supported with only 1DOF and $m^* = 5.3$ (relation between structural mass in oscillation and displaced mass of fluid)[1] have shown that the maximum transverse amplitude increases with an increasing of the Reynolds number in the range from $2.0 \cdot 10^2$ to $1.0 \cdot 10^5$, a behavior previously discussed in Govardhan and Williamson [26]. Moreover, the lower branch gradually ceases to exist for the largest Reynolds numbers, as also reported in Raghavan and Bernitsas [46] by means of experiments with horizontal cylinders elastically supported in 1DOF. In [2], it was shown that transverse amplitude maximum drops by a factor of 2 when the surface roughness was increased from $k/D = 1.0 \cdot 10^{-5}$ to $5.0 \cdot 10^{-3}$ at Reynolds number of approximately $1.40 \cdot 10^5$. This probably comes from changes in the boundary layer and it supports the usual procedure for small-scale tests of floating units.

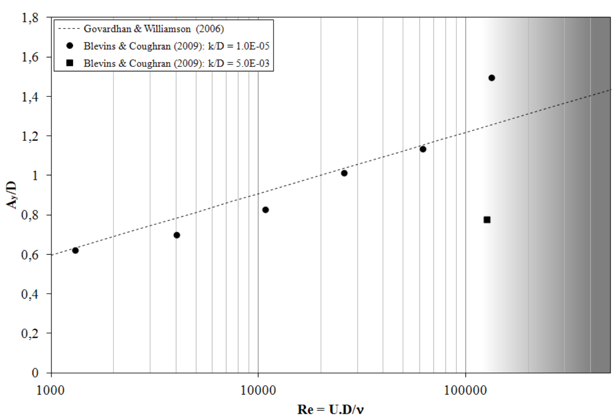

FIGURE 3: Maximum transverse amplitudes as function of the respective Reynold numbers. Experimental results adapted from [2] and theoretical result plotted according to [26].

When taking into account the concerns presented in Yung et al. [68] and Ding et al. [7], the last one particularly pointing out the complex nature of the VIM dependence on Reynolds number and surface roughness, the procedure herein discussed is certainly the only one feasible in most of the facilities available. Additionally, recent results found by Roddier et al. [50] from a series of model tests with only the hard tank of a spar platform ($L/D = 1.7$), in three different Reynolds regimes (three different facilities), reveal that:

1. Tests at subcritical regime are acceptable and slightly conservative;
2. Small-scale tests of floating units are a good solution for considering the VIM effects in a reliable way;
3. There are little difference at reduced velocities higher than 7 between small-scale tests at subcritical and supercritical regimes, remarkably achieved by applying the Froude scaling in terms of geometrical and dynamic similarity.

Degrees-of-freedom The ability of oscillating in more than one degree-of-freedom plays an important role in VIM response of floating units, see for instance Fig. 4 for the importance on the fatigue life of risers and mooring lines. However, there is not much specific research on this issue for platforms and, consequently, much of the remarks concerning it are based on the VIV phenomenon acting on cylinders with only 2DOF, where it is well known that the simple coexistence of oscillations transverse and in-line to the fluid flow brings striking changes to the dynamic behavior. That is why the fundamental approach herein presented is focused on VIV of cylinders with 2DOF.

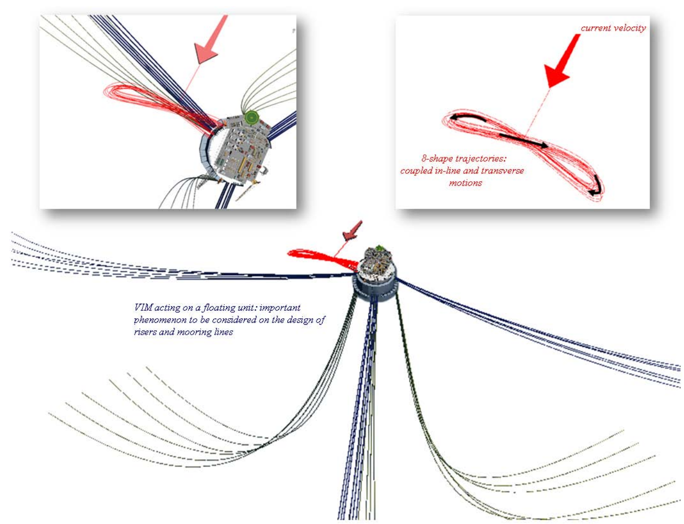

FIGURE 4: The 2DOF play an important role on VIM response of floating units.

Some of the earliest studies on VIV response of cylinders with 2DOF are found in King [35] and Chen and Jendrzejczyk [3], particularly focused on the phenomenological aspects of the coexistence between transverse and in-line oscillations. According to theoretical and experimental considerations, those works

[1]This parameter has a strong influence on response due to VIV or VIM and it will be discussed in next section.

clearly state the existence of two synchronization regions, see Figure 1 (upper plot), the first region being related to the in-line oscillations, for $2.5 < V_r < 4.5$, and the second one to the transverse oscillations, for $V_r > 4.0$. Some dependence on the damping coefficient with respect to the flow velocity is reported in [3].

Sarpkaya [54] compared experiments with cylinders free to oscillate in 1DOF and 2DOF. According to that work, the cylinder free to oscillate in both directions is able to exhibit coupled motions, sometimes in *8-shape*, featured by transverse amplitudes 19% higher than that from cylinders with only 1DOF, and strongly dependent on the ratio between the natural frequencies in-line and transverse to the fluid flow. Moreover, the case of 2DOF has provided a maximum amplitude at a slightly higher reduced velocity, with no evidence of being assigned to any other branch of resonance. Some years later, in Pesce and Fujarra [44], a long and flexible cylinder was towed in a cantilever condition, showing a similar behavior to that observed in [54]. Moreover, an overlapping between two stable response branches in the range of $6.5 < V_r < 8.0$ was observed, including records of a jump phenomenon between those branches, where the upper one was clearly featured by motions in *8-shape*.

Those results were confirmed in Fujarra et al. [16], where the VIV phenomenon was investigated in two different water channels, at University of Michigan and Cornell University, based on another flexible cylinder presenting a mass ratio of $m^* = 1.30$, as well as a ratio between natural frequencies of $f_{nx}/f_{ny} = 4$ (f_{nx} and f_{ny} respectively related to the in-line and transverse direction). Again, a remarkable overlapping between two stable branches of response was observed, although without such high amplitudes like those observed in [44]. The behavior was assigned to the different ratios of natural frequencies and also to the higher damping coefficients tested. Although not fully conclusive, the results from [54], [44] and [16] clearly show the importance of the coexistence between in-line and transverse oscillation for the VIV phenomenon, and consequently for the VIM, providing a starting point to the researches developed later, considering circular cylinders with not only 2DOF, but also with small mass ratio and low damping coefficient.

Investigations to assess the effect of Reynolds number on the VIM response of floating units have been made mainly through two kind of experimental setups at towing tanks, each one with particular advantages and drawbacks. The first one, for instance found in Yung et al. [68] and Kokkinis et al. [36], is featured by a fully submerged double-body model supported in horizontal position by a self-controlled actuator free to oscillate only transverse to the fluid flow. This setup gives precise measurements of the force for larger models and is able to compensate the mechanical damping, making it possible to evaluate the impact on the VIM phenomenon. Unfortunately, although the advantages, its construction didn't permit the evaluation of the important coexistence between in-line and transverse motions. The second kind of experimental setup is based on floating models connected to the towing carriage through combinations of cables and springs, as described for example in [9], [61], [60], [10] and [50]. This setup has great similarity to the full scale configuration, including the ability to capture some non-linear effects coming from the restoring system, as it presents 6DOF. The floating model can be evaluated not only in term of its performance due to VIM, but also in a simultaneous occurrence of waves. For a accurate design of the restoring system, it is necessary to take into account not only the stiffness, but also damping problems, movements and perturbations of the restoring lines. Forces and moments are more difficult to measure in this setup, particularly because they are prone to a larger number of uncertainties.

Mass ratio Based on the studies developed by Jauvtis and Williamson [33] and Williamson and Jauvtis [66], part of the aspects concerning the VIV phenomenon and its dependence on some parameters were understood according to a better phenomenological approach. The mass ratio was the first of these parameters, being defined as a relation between the structural mass in oscillation, m_s, and the fluid mass displaced by the cylinder, m_f, see eq. (3).

$$m^* = m_s/m_f \tag{3}$$

Through experiments in a water channel considering different values of the mass ratio, two different dynamic behaviors for cylinders with 2DOF were recognized. The first behavior was associated with cylinders with *moderate to large mass ratios*, $m^* > 6$, presenting similar response to that of 1DOF cylinders. Another behavior was related to cylinders with *moderate to small mass ratios*, $m^* \leqslant 6$, being similar to that reported in [16]. For this last behavior, in-line and transverse oscillations were simultaneously identified, revealing a new stable branch of response, related to a triplet of vortices being formed in each half-cycle of oscillation and defined as a *"2T"* mode of shedding. The so termed *Super Upper branch (SU-branch)* in Figure 1 was featured by oscillations in *8-shape* of high maximum amplitude, approximately $1.5D$ in the transverse direction. The *SU-branch* is also more stable and more periodic. In Jauvits and Williamson [32], the importance of the mass ratio was accurately defined, presenting $m^* = 6$ as a limit value for identifying the *SU-branch* on the transverse response of 2DOF cylinders, and $m^*_{crit} = 0.52$ as a critical value below which the *Lower branch (L-branch)* ceases to exist, even for higher reduced velocities. In fact, Morse and Williamson [38] have recently shown that m^*_{crit} strongly depends on the Reynolds number, at least for a bare cylinder with 1DOF, lightly damped and in the range of $4.0 \cdot 10^3 < Re < 3.0 \cdot 10^4$.

By means of a force assisted apparatus, in Dahl et al. [5] a rigid cylinder was investigated in the towing tank at MIT. The

VIV phenomenon was studied according to six different ratios of natural frequencies, f_{nx}/f_{ny}, respectively related to low damping coefficients from 0.0011 to 0.062; those values being achieved via linear motors working in a self-controlled manner in order to compensate the damping of the elastic support. Moderate mass ratios were considered, varying from 3.3 to 5.7. According to the results, the phase angle observed between the coupled motions from VIV is strongly affected by the in-line value of the natural frequency, f_{nx}, which has impact on the maximum amplitude of transverse motion. Moreover, the reduced velocities corresponding to the maximum transverse amplitude was changing to higher values when the in-line natural frequency was increased, also confirming the results recognized in [54], [44], [16] and [45] for cylinder with 2DOF and small mass ratio.

In Dahl et al. [6], details concerning the vortex shedding patterns due to VIV were discussed through comparisons between experimental and numerical results achieved by considering cylinders with 2DOF. It was shown that, depending on the ratio between the natural frequencies, fundamental changes in the 2DOF trajectories and in the frequency spectrum of the related fluid forces occured, which are caused by one (or a combination) of the following reasons: (a) stable and periodic shedding patterns of multiple vortices, being generated instead of the patterns recognized for transverse oscillations, *2S - two single vortices* or *2P - two pair of vortices*; (b) stable motion in *8-shape* and counter-clockwise direction, whereby the cylinder moves upstream just before the vortices are shed, and then moves downstream, going against the recently shed vortices approximately at the center of the trajectory. As a result, the 2DOF cylinder may experience strong fluid forces due to the shedding of multiple vortices, resulting in lift forces at high frequency. Therefore, the lift force may not be always related to the fundamental frequency of shedding, approximately equal to the Strouhal frequency, may come from components significantly higher in frequency.

Concerning the implications of the *SU-branch* for the design of floating units, usually featured by small mass ratios and at least 2DOF, experiments with a vertical cylinder elastically supported were performed in Stappenbelt and Lalji [57], seeking to understand the coupled motion due to VIV under different values of the mass-damping parameter, $0.014 \leqslant m^*\zeta \leqslant 0.078$. According to that work, the damping coefficient plays an important role for the VIV response and the mass-damping parameter should be considered for defining the limit of existence for the *SU-branch*. Actually, for $m^*\zeta > 0.066$, very similar results between cylinders with 1DOF and 2DOF were obtained, with a gradual coalescence between the response curves as a function of increasing mass-damping parameter.

Searching for the impact of changing parameters like mass ratio, damping coefficient and Reynolds number, a series of experiments comparing cylinder with 1DOF and 2DOF were performed by Blevins and Coughran [2], comprising cases of mass ratio varying in the range of $1.00 \leqslant m^* \leqslant 11.00$, damping coefficient in the range of $0.002 \leqslant \zeta \leqslant 0.400$, reduced velocities varying from 2 to 12 and Reynolds number up to $1.50 \cdot 10^5$. The main results were:

1. By increasing the damping coefficient for a mass ratio of $m^* = 3.20$, smaller oscillations in the transverse direction were observed, presenting maximum values of amplitude in reduced velocities gradually lower;
2. A second set of experiments was performed by considering a fixed damping coefficient of $\zeta = 0.020$ and different values of mass ratio. The results for $m^* > 1.0$ were quite similar to those discussed by Jauvits and Williamson [32], particularly concerning the qualitative response of VIV, which means the presence of both branches for responses associated with the longitudinal oscillations at $2 \leqslant V_r \leqslant 4$, *i.e. Streamwise Symmetric (SS-branch)* and *Streamwise Antisymmetric (AS-branch)*, as well as all the branches coming from the transversal oscillations for reduced velocities up to approximately 12, *i.e.* the *Initial*, *Upper* and *Lower branches (respectively, I-branch, U-branch and L-branch)*. Like previous works, a branch of coupled movements in *8-shape* and high amplitudes in the transverse direction was recognized, without discussing the pattern of shedding responsible for it. For increasing mass ratio, the coupled motions ceased to exist at lower values of reduced velocity. Conversely, by decreasing the mass ratio, the *I-branch* appeared gradually at lower reduced velocities.
3. The results of Blevins and Coughran [2] for 2DOF considering $m^* = 1.0$, $\zeta = 0.063$ and aspect ratio[2] of 13.0 seem to be the first in the literature. Although not conclusive, a continuous increasing of the transversal oscillation was pointed out with no evidence of the *L-branch*. The same behavior was presented in [57] by means of the critical value for the mass-damping parameter and quite close to the response recognized for the VIM measured in small-scale experiments of floating units.

Recently, in Gonçalves et al. [22], cylinders with 2DOF and very low aspect ratio, $L/D \leqslant 2$, were investigated in terms of VIV response and compared to the previous results from structures with approximately the same mass ratio. Figure 5 is an example for structures with $2.36 \leqslant m^* \leqslant 2.80$. As can be seen, great part of the phenomenology is kept independent from the nature of the structure, even considering a flexible cylinder with aspect ratio of 94.5, from ref. [44], cylinders elastically supported with 2DOF and aspect ratios between 8 and 18, from ref. [32], [57] and [2]; or also a cylinder with an aspect ratio of 22 and supported by a 2DOF pivoted bar, from ref. [15].

Actually, by comparing the transverse amplitude from Gonçalves et al. [22] and Stappenbelt and Lalji [57] as function

[2] Another important parameter for VIV or VIM. Also, it will be discussed in the next section.

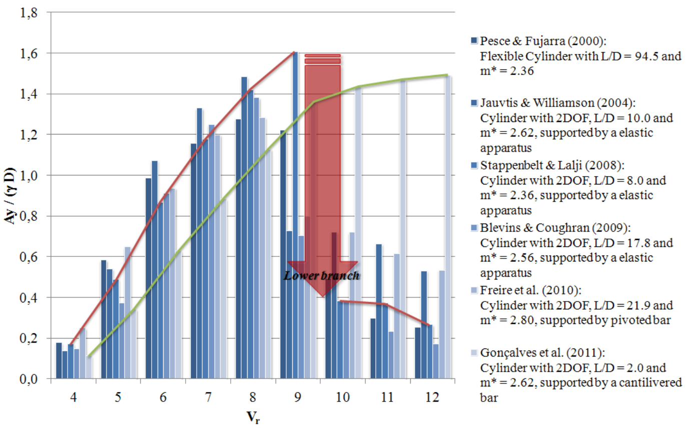

FIGURE 5: Comparison between nondimensional transverse amplitude as function of reduced velocity for different apparatus with similar mass ratios.

of the reduced velocity, leads to the green and red lines in Fig. 5. It can be observed that there are two main differences between the short and the long cylinders with practically the same mass ratio, respectively 2.36 and 2.62. The first one concerning the shift for higher reduced velocities, as reported in [54] and [2], and the second one concerning the absence of the *L-branch* in the case of very short cylinders. Regardless the short aspect ratio, the transverse amplitudes reported by Gonçalves et al. [22] are quite the same, which supports the assumption that not only the mass ratio but also the aspect ratio plays a important role in the dynamics of floating units due to VIM.

Aspect ratio Regarding the influence of the aspect ratio on the VIM phenomenon, it can be observed that most of the available studies are related to fixed cylinders under the effect of a free end. Very few results are found concerning the effects of the aspect ratio on the dynamics of a floating body, even considering studies in lower values of Reynolds numbers.

Usually defined as the relation between the effective immersed length (the draft for the floating units) and the dimension of the cross section (the hydrodynamic diameter of the cylindrical body), see eq. (4), the aspect ratio is responsible for controversial issues related to its influence on the fluid-structure interactions. The most important ones are presented here in order to highlight possible effects for full scale problem of floating units.

$$A_R = L/D \tag{4}$$

It is a matter of consensus that the frequency of vortex shedding decreases as the aspect ratio is decreased, as originally discussed in Okamoto and Yagita [41]. Moreover, one can define a critical value of $(L/D)_{crit} \cong 2.0$, see Sakamoto and Arie [53], according to which the flow model downstream of a rigid and fixed cylinder can change drastically. According to Kawamura et al. [34], two flow models around finite cylinders are presented taking into account $(L/D)_{crit}$. For aspect ratios above 2.0, the existence of a *von Kármán* vortex shedding is proposed, adjacent to the region affected by the downwash effect promoted by the trailing vortices near the free end. For aspect ratios below 2.0, another flow model is proposed, where the *von Kármán* vortex shedding ceases to exist.

The first controversial issue concerns the existence, or not, of the trailing vortices at the free end of the fixed cylinder. According to [41], a gradual delay on the *von Kármán* vortex shedding near the free end becomes present, resulting in a continuous line of vortices properly inclined and attached to the free end. For cylinders with aspect ratio below the critical value, it is shown in [53] that an *arch-type* shedding takes place instead of the *von Kármán* vortex shedding. On the other hand, recent studies such as those in Park and Lee [43], Roh and Park [51], Sumner et al. [58] and Rödiger et al. [52] have given strong evidence of the trailing vortices, however, without a topological explanation for their interaction with the *von Kármán* vortex shedding near the free end. In [51], a vortical structure comprising of two pairs of counter-rotating vortices at the free end of a rigid and fixed cylinder is proposed, being responsible for the downwash effect in the wake. Details about the topological interaction between the trailing vortices and the *von Kármán* wake are presented in Palau-Salvador et al. [42], recently obtained by using a combination of experiments and Large Eddy Simulation (LES) for cylinders with $L/D = 2.0$ and 5.0.

Regardless of the vortical structure downstream of finite cylinders, it is quite clear that the different types of flow are responsible for changing the Strouhal number along the cylinder. However, it is not yet clear how it happens. Investigation based on measurements of the velocity field, such as those in [41], proposes the existence of a gradual decreasing of the Strouhal number toward the free end of fixed cylinders, with lower values found between $2D$ and $4D$ and with zero values for distances smaller than $2D$. In Ayoub and Karamcheti [1] it was suggested that an unstable and intermittent vortex shedding process inside this latter region exists, making it difficult to define a Strouhal number for this case. Conversely, investigation based on pressure measurements on the surface and also by means of fluctuations in the lift force, like those found in Farivar [8], Fox and West [13][14] and Fox and Apelt [12] have reported a Strouhal number varying in steps toward the free end as a consequence of cellular structures in the vortex shedding.

Despite the controversies about the vortex shedding downstream fixed cylinders, the following question can be posed: *Why shouldn't it be also expected that a complex behavior exists near finite cylinders free to oscillate, such as spar and monocolumn* *platforms?* A first answer comes in Nakamura et al. [40], where the in-line oscillations of a elastically supported rigid cylinder were investigated as function of the aspect ratio, $L/D \geqslant 5.0$. According to the experimental results in a water tunnel, the aspect ratio changes the transition between the resonant regions in the fluid flow direction (from the *SS-branch* to the *AS-branch* of vortex shedding, see Fig. 1, originally described in [35]), but it doesn't change the maximum amplitude of in-line oscillation. Furthermore, in Morse et al. [39], the free end effect was investigated considering a rigid cylinder with $8D$ in length and free to oscillate only in the transverse direction. Against the expectation, the transverse amplitudes of oscillation for the cylinder equipped with an endplate were not higher than those presented by the same cylinder without that device. Apart from those previous researches, only in Someya et al. [55] the first results of VIV on short cylinders with 2DOF are found, unfortunately, only for reduced velocities up to 4. Some decisive evidences are given in Gonçalves et al. [22], where cylinders presenting 2DOF kept the vortex shedding resonance even for lower aspect ratios, remarkably similar to that usually found for long cylinders.

COMPREHENSIVE SURVEY ON VIM EXPERIMENTAL RESULTS

Keeping in mind the discussion presented above, we now discuss the particular aspects concerning the dynamic behavior of the VIM phenomenon acting on spar, monocolumn, semi-submersible and tension-leg platforms, see Fig. 6.

In order to make easy comparisons and take some general conclusions, all data found in the open literature were organized in Tabs. 2, 3, 4(a) and 4(b). Table 2 brings the main characteristics and conclusions obtained by small-scale tests or field measurements of spar platforms. Table 3 presents data gathered from tests with monocolumn platforms. Tables 4(a) and 4(b) presents data for semi-submersible and tension-leg platforms. Chronological order of appearance in the open literature is adopted, although for the sake of conciseness some related works have been grouped in a same row.

It is important to point out that such a division was also motivated by particulars of each kind of floating unit, some of them very distinct from each other. It is remarkable that, as a consequence of the problems on the Genesis spar platform, most of the works in the first years of VIM investigation were focused on technological solutions for the observed problems. Only recently, the experimental investigation adopted a more fundamental approach in terms of the main aspects presented in the background section.

VIM acting on spar platforms

Table 2 summarizes parameters and characteristics of tests conducted by means of three types of spar platforms: classic, truss or cell; see differences in Fig. 7. Each row represents an experimental investigation, arranged in chronological order of appearance in the open literature and identified by references in the first column of the table.

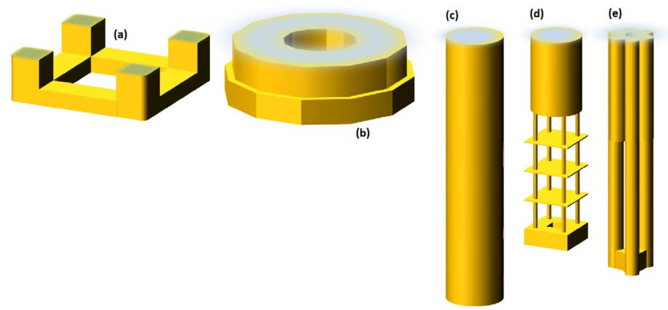

FIGURE 6: Comparison between geometries able to present VIM: (a) semi-submersible; (b) monocolumn; (c) classic spar; (d) truss spar and (e) cell spar platforms.

The spar platforms investigated by each research are presented in the second column, together with the scale factor, λ (highlighted in red). One can note that $22.3 \leqslant \lambda \leqslant 142.8$, with a large number of investigations performed considering a scaling factor around 50, such as for example in [9], [11], [29], [60] and [61]. Regarding the wide range of scale factors and possible concerns about scale effects on experimental results of VIM tests, as pointed out by van Dijk et al. [60], a thorough investigation was recently performed by Finnigan and Roddier [10] and Roddier et al. [50]. According to their experiments in three different towing tanks, slightly different results were observed taking into account the same hard tank of a truss spar in three appropriate scales (22.3 in David Taylor Model Basin, 65.0 in Force Technology Tank at Denmark and 142.8 in University of California at Berkeley). Considering the wide range of Reynolds numbers tested, $4.1 \cdot 10^4 < Re < 1.6 \cdot 10^6$, it was possible to state that testing at subcritical region is acceptable and slightly conservative for design purpose, presenting small differences compared to the supercritical region, particularly when $V_r \leqslant 7$. As discussed before in terms of the infrastructure limitation (length and possible velocities in the towing tanks), for most of the investigations the Reynolds number varies from 10^4 to 10^5.

Although presented as an important effect, the surface roughness of the model is only thoroughly discussed by van Dijk et al. [60], certainly because all the experiments have considered a great number of appendices (such as anodes, fairleads, chains and pipes), hypothetically enough to emulate the turbulent boundary layers present in full scale. More details about this issue will be discussed from the experiments with monocolumn platforms.

The third column of Tab. 2 describes characteristics of the applied infrastructure, particularly regarding the experimental

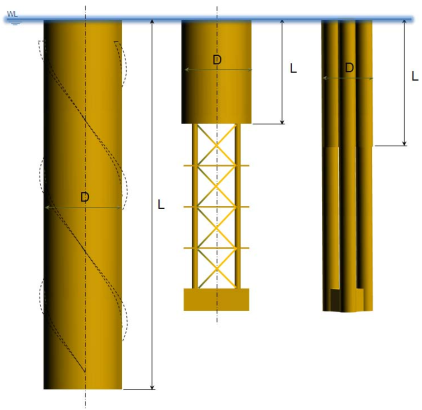

FIGURE 7: From left to right: the classic, truss and cell geometries of spar platform. For each geometry, the main considered parameters are presented: effective immersed length, *L*, and hydrodynamic cross section, *D*.

basin and how the small-scale models were supported during the tests. Most experiments were performed in towing tanks, considering small-scale models floating on the free surface, *i.e.* presenting 6DOF. However, some researches were performed in flume or offshore basin, such as those respectively presented in [9] and [11]. According to Finn et al. [9], VIM results obtained from towing tank and flume are comparable. A similar conclusion is presented in Finnigan et al. [11], with the additional advantage for flume tests regarding the possibility for emulating current profiles of long term, not only uniform, and also for acquiring long records of measurement for better statistics.

Experiments based on a double model horizontally supported are only found in [36] and [68]. Despite its clear advantage for high Reynolds numbers, small effects from the free surface and damping control, this kind of apparatus provides only 1DOF, what is not enough for getting reliable responses due to VIM phenomenon, usually featured by coupled motions in the free surface (generally trajectories in *8-shape* with higher response amplitudes).

The nature of the experimental stiffness is another aspect covered by the survey summarized in Tab. 2. Based on works which consider floating models, there are three main types of restoring system for the small-scale tests. The first one is featured by cables and equivalent springs, assembled horizontally with three or four lines (sometimes slightly inclined or even presenting a soft catenary), depending on the full scale mooring system design of the floating unit under investigation. Restoring systems like this are found in [10], [11], [50], [60], [61] and [63]. Another restoring system applied in VIM tests is a truncated version of the complete mooring system, *i.e.* catenary or semi-taut mooring lines, for instance found in [61], [64] and [65]. Because of its non-linear character, it is applied for tests under a possible variation of natural periods and added mass (mainly in surge and sway directions, as consequence of the large offset due to the drag load), usually required for advanced phases of analysis. The last generally used restoring system for VIM tests is based on hanging weights, combining the easy and shallow installation with the non-linear possibility of restoring. The restoring force is linearly proportional to the hanging weight and is a function of the offset, having the non-linearity determined by the geometry of each line. This kind of system was used in [9] and [29], where the experimental stiffness can be easily adjusted, by increasing or decreasing the size of the hanging weights.

According to comparisons performed in van Dijk et al. [61], it is important to emphasize that horizontal equivalent restoring systems (based on linear springs and cables) are a good alternative for VIM tests. This is why most of the experimental investigations use this type of restoring for towing the small-scale model at the free surface.

The unique characteristic of each experimental investigation on VIM of spar platforms prohibits any conclusion regarding the dependence of the maximum transverse amplitudes with the aspect ratio, A_y/D as function of L/D (see Fig. 7 for definitions herein adopted), although it had been pointed out in some fundamental studies on VIV phenomenon. Some qualitative results can be found in Wang et al. [63]. Many works have performed numerical simulations based on the Computational Fluid Dynamic – CFD approach, but no one in a complete and reliable stage to bring the necessary comprehension regarding this issue. Nonetheless, the following behaviors are observed for spar platforms.

Since spar platforms are covered by appendages, the heading plays a important role on VIM response. It is responsible for changing the correlation between in-line (surge) and transverse (sway) motions, in some cases featured by trajectories in *8-shape* and higher amplitudes, as those reported for example in [60] and [63].

The synchronization region is another characteristic strongly affected by the geometry of the platform, not in terms of the beginning (typically between reduced velocity of 4 and 5), but concerning where it ceases to exist. As reported for example in [64], there are some cases where the synchronization region seems no longer be maintained for reduced velocities greater than 10.

Strakes are usually applied for mitigating the VIM on spars and deserve extreme attention, since their effectiveness depends on many aspects related to the platform. As stressed by [29], care should be taken regarding how to present results of VIM on straked models, since a spar platform covered by strakes of height h will present nondimensional amplitudes more related to $A_y/(2h+D)$, where D is the hydrodynamic diameter of the unstraked spar. Taking this into account, strakes of height around $14\%D$ seem to be more effective to suppress the VIM phenomenon, as discussed for example in Wang et al. [65], with no consensus regarding the number of starts (3 or 4) and pitch, both aspects depending on the spar geometry, its mooring system and the excitation conditions.

The effect of different current profiles on the VIM response of a truss spar was initially investigated in van Dijk et al. [61], comparing a *hurricane current profile* (one uniform velocity acting on the hard tank and lower sheared profile on the truss below it) and a *loop current profile* (uniform over practically the whole draft, and sheared below it). The first main conclusion was about the effects posed by the highly sheared current profile, particularly related to the turbulence frequencies near the natural frequencies in-line and transverse to the current, capable to excite significant in-line motions. Besides that, some differences were observed on the drag loads and damping due to the truss, which was not fully investigated and was highlighted as an aspect to keep under consideration. Finnigan et al. [11] mention the possible influence presented by the truss in terms of its effect on the VIM response. Two current profiles were tested, the first one uniform over the whole spar draft and the second uniform over most of the spar hard tank and practically zero below it. Comparing the VIM results from those profiles, no significant differences were observed between sheared and uniform current flow.

The first attempt of considering the simultaneous excitation of VIM and waves is found in [11]. According to this work, a truss spar under exclusive excitation of current has maximum transverse amplitude of 0.23 at a reduced velocity of approximately 7. On the other hand, when it is submitted to simultaneous irregular waves in the same direction, the response of VIM was drastically reduced, reaching a maximum value of $A_y/D = 0.07$. Other incidences of irregular waves, transverse and oblique to the current, were tested without significant reduction of the VIM phenomenon as observed before.

Finally, an important comparison between design predictions and field measurements for a truss spar is presented in Irani et al. [31]. According to the authors, the field measurements of VIM response presented a maximum transverse amplitude of approximately 0.26, considerably lower than the values predicted during the design phase, 0.50. As a consequence, it is postulated that design values can only be evaluated after extensive experimental investigation, deserving extreme care regarding the uncertainties when extrapolating the small-scale results to the full scale condition.

VIM acting on monocolumn platforms

The meaning of a monocolumn platform herein adopted is that of a round Floating, Production, Storage and Offloading – FPSO systems similar to that presented in Fig. 8. In 2007, the first monocolumn platform was installed offshore the Sergipe state in Brazil. Named *Sevan Piranema*, it is an unit of $60m$ in diameter at the waterline, $18m$ draft and $55,000ton$ displacement. After that, two similar monocolumn FPSO systems have been installed: the *Sevan Hummingbird* in 2008, at Chestnut field, and the *Sevan Voyageur* in 2009, at Huntington field, both situated in UK North Sea.

Beside those projects, in Brazil, since 2001 a technical agreement between Petrobras and the University of São Paulo, as well as many other R&D projects, have investigated this concept in a wide range of geometries, applied for different locations in Brazil and the Gulf of Mexico. Some of them with a displacement greater than $250,000ton$ and moonpools, beaches, skirts and spoiler plates, which results in small vertical motions for operation of steel risers and dry completion systems. More details can be found in Gonçalves et al. [20].

Table 3 summarizes the main parameters and characteristics of small-scale tests conducted for the FPSO monocolumn platforms.

By inspecting the facility information and number of degrees-of-freedom, one can realize that all the experimental investigations on VIM of monocolumns were performed on small-scale models, floating at the free surface and towed by means of a horizontal mooring system. The scale factors adopted also deserves attention, since they are greater than those adopted for spar models, $90 \leqslant \lambda \leqslant 200$. This is a consequence of the very large diameters involved and restrictions imposed by the infrastructures. However, similar behaviors to those gathered from spar platforms can also be identified for the VIM of monocolumn platforms.

Firstly, the increase of surface roughness is investigated in Cueva et al. [4] for VIM tests of a monocolumn designed for operating at Gulf of Mexico current conditions. Likewise as for spar platforms, sufficient roughness was able to emulate a supercritical regime at Reynolds numbers varying from $2.0 \cdot 10^4$ to $1.0 \cdot 10^5$, keeping the drag coefficient approximately constant for all tested velocities. In Gonçalves et al. [19] and [25], the same result is achieved by means of a new series of tests at different

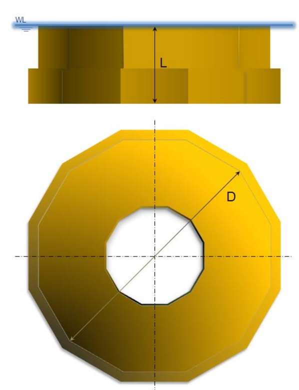

FIGURE 8: Main parameters for monocolumn platforms: effective immersed length, L, and hydrodynamic cross section, D.

facilities. A good repeatability of the VIM was obtained for the tests with added surface roughness.

Another aspect confirmed by the VIM tests on monocolumn platforms refers to the importance of heading. Again, appendages such as anodes, fairleads, chains, risers support and pipes play a important role on the response amplitude behavior. For instance, pipes placed vertically on the immersed hull surface can provide a separation point for the boundary layers and, consequently, a more correlated vortex shedding mechanism. The *Sevan Piranema* monocolumn investigated in Fujarra et al. [17] is fitted with a huge support for risers, placed in part of its circumference. Depending on its heading, such a structure is responsible for a large asymmetry on the wake, sometimes without visible spanwise correlation.

Keeping in mind the spanwise correlation of vortex shedding, it is curious how such type of platform is also susceptible to VIM, for very low aspect ratios of $L/D < 0.50$ in all units, as presented in Tab. 3. This leads to the two flow models described in Kawamura et al. [34], concluding that a *von Kármán* type vortex shedding should not exist for aspect ratios below $(L/D)_{crit} \cong 2.0$. However, it is important to remember that the critical aspect ratio proposed in Sakamoto and Arie [53] is related to the fluid flow passing on fixed cylinders. According to the recent evidences presented in Nakamura et al. [40] and Someya et al. [55], free cylinders must present drastic changes in terms of flow models, unfortunately not fully described, but which can justify those high response amplitudes as consequence of the VIM phenomenon acting on the low aspect ratio of floating platforms. In Gonçalves et al. [21] the decrease in draft is pointed out as the most decisive effect to mitigate VIM on monocolumn platforms. A result that agrees with the hypothesis of a weak spanwise correlation, deeply affected by a tridimensional shedding coming from the free end of the floating body.

An usual behavior identified from the results of VIM on monocolumns is the remarkable existence of coupled motions in *8-shape*, which are responsible for sustaining the response amplitudes higher than unity for reduced velocities greater than 8. For some experiments, like those presented in Cueva et al. [4], an end for the synchronization region was not observed. That is why tests with $V_r > 12$ are necessary to identify a potential synchronization with higher response amplitudes, particularly important for softer mooring systems and for high flow velocities. In [4], a set of spoiler plates is proposed for suppressing VIM on monocolumns. Arranged according to three helical starts, they were responsible for dramatically reducing the VIM amplitudes. Similar to what happens with the strakes on spar platforms, it is stated that an ideal arrangement of spoiler plates has strong dependence on the shape of the monocolumn, justifying additional experimental investigation, possibly supported by means of properly conducted CFD simulations.

As pointed out by Irani and Finn [30], with suppressing devices, such as strakes and spoiler plates, the VIM response becomes more modulated in terms of the time histories, which deserves attention in defining the maximum amplitude. In Fujarra et al. [17], the Hilbert-Huang Transform – HHT is presented as an innovative technique for signal processing of VIM tests, obtaining better statistics even for short time histories, sometimes modulated in amplitude. Details about the HHT technique and its comparison to the classical FFT can be found in Gonçalves et al. [24].

Two final subjects related to monocolumn platforms are the interaction of VIM and waves and the VIM behavior in the presence of extra damping from the risers. It is well known that the simultaneous excitation coming from current and waves plays a important role, as originally investigated in Finnigan et al. [11] for a truss spar platform. In Fujarra et al. [18] and [21], regular waves with periods close to the natural period of heave were able to mitigate VIM acting on MonoBR, probably indicating that the simultaneous resonance in vertical direction suppresses the correlated shedding mechanism of the vortices. Regarding the effect coming from the extra damping due to riser system, [18] and [21] show that a higher damping emulating the presence of risers is capable to change substantially the VIM responses.

VIM acting on semi-submersible and tension-leg platforms

The VIM on Semi-Submersible – S-S and tension-leg platforms – TLP has become an important issue in the last years, particularly due to the deep draft and higher natural periods presented by the new developments. Considering units such as that schematically represented in Fig. 9, one can expect a dynamic behavior considerably more complex as a result of interactions between wakes coming from the multiple columns. Tables 4(a) and 4(b) summarize the main parameters and results gathered from ten VIM tests on small-scale models of semi-submersible and tension-leg platforms. Some results from field measurements are also considered.

All collected data relate to deep draft S-S or TLP with four square columns and rounded corners, except for one where columns are made up of four tubes. Both two and four box shaped pontoons were considered. For convenience, the following acronyms are used in the refereed tables: $[4Sc\&4Bp]$, $[4Sc\&2Bp]$ and $[4x4Tc\&4Bp]$. The diversity in geometries tested can be seen by comparing the nondimensional parameters: H/L, S/L and H/P, see Fig. 9. Important to emphasize that no attempt was made to relate these parameters with the VIM behaviors.

All models were scaled in the range $48 \leqslant \lambda \leqslant 100$, with a concentration at $\lambda \cong 50$. Effects arising from the scale factor were not investigated. Concerning the Reynolds numbers, all the small-scale models were tested in the subcritical region and no added surface roughness was considered, since square columns and a number of appendices are enough to emulate the turbulent boundary layers present in full scale.

All the experimental investigations were performed in towing tanks, except for the studies found in Hong et al. [27] and Stansberg [56], where VIM and wave excitation were investigated simultaneously in an ocean basin (more details related to this issue are given further on). For the towed cases, all the models were free to oscillate in at least the plane of the free surface, *i.e.* in-line and transverse to the flow current (surge and sway, respectively), as well as rotate (yaw). In Waals et al. [62] and Rijken et al. [49], a device based on air bearings was used to provide vertical pretension. In fact, that device was designed for TLP tests. For all the other cases, a floating model is the usual solution.

Regarding the nature of the experimental stiffness, most of the experiments were based on a system of 4 horizontal equivalent springs, like in Gonçalves et al. [23], Magee et al. [37] and Rijken and Leverette [47]. Additionally, experiments found in Rijken et al. [49] consider not only the system of 4 horizontal equivalent springs but also 2 extra springs for emulating the stiffness coming from steel catenary risers. Even considering the extra stiffness, no changes were noticed on the VIM behavior, because of its lower magnitude compared to the equivalent mooring stiffness. Similar investigation is also found in Tahar and Finn [59], but based on 4 taut lines and an extra line simulating the presence of risers. Again, nothing is reported in terms of a substantial difference on the VIM behavior due to the extra stiffness. Other experimental stiffness systems are found in Hong et al. [27], based on 4 truncated lines in a catenary geometry; in Hussain et al. [28], considering 12 truncated lines coupled to mechanical actuators by cables and linear springs; and in Stansberg [56] by means of a 12-leg catenary system. Despite those different systems, only concerns about the frequency of vortex shedding and natural frequencies are presented, without conclusive discussion on the effects from the stiffness on the VIM responses.

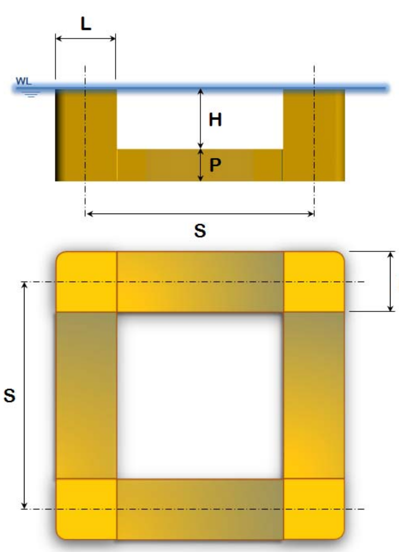

FIGURE 9: Main parameters for semi-submersible and tension-leg platforms: effective immersed length of the column, H; face dimension of the column, L; height of pontoons, P and distance between columns, S.

The most striking results from VIM tests of TLP and S-S platforms come from heading sensitivity. Platforms with four columns have the largest transverse amplitudes when positioned with 45 degrees of heading. Waals et al. [62] have shown that the effect of mass ratio on VIM of floaters is consistent with that observed for VIV on long cylinders; see Rijken and Leverette [47]. The range in which the synchronization occurs is larger for flow angles smaller than 45°, but related with smaller transverse amplitudes. According to Gonçalves et al. [23], the transverse synchronization can occurs for reduced velocities from 4 to 14 depending on the heading. In Magee et al. [37], similar behavior of a wider range of synchronization is reported, as well as it is observed that draft changes affect the VIM response more at 45° than at 0°. Finally, Tahar and Finn [59] show that the drag coefficients appear to be in constant relationship to the response amplitudes.

The nondimensional amplitudes refer to nominal values, defined as $A_y/L = \sqrt{2} \cdot std\,\{y(t)\}$ in Tabs. 4(a) and 4(b), where: L is the face dimension of the column and $y(t)$ is the displacement time history in transverse direction.

Regarding the effects of heading, large yaw motions at higher reduced velocities were reported in [23], [28], [37] and [62]. Originally observed in Waals et al. [62], those yaw motions were related to a possible phenomenon of galloping. On the other hand, by performing a complete set of analysis in the frequency domain (via FFT and also HHT technique), in Gonçalves et al. [23] the yaw motions are described as a resonance behavior similar to the VIM in the transverse direction (sway). Whatever its nature, the yaw-VIM is more presented on TLP and S-S platforms, with larger angles related to the 0° of heading, as observed by Hussain et al. [28] and Magee et al. [37].

Appendages such as anodes, fairleads, chains and pipes play a important role in terms of heading, especially when located on the vertical faces of the upstream columns and above the pontoon level, as suggested in Rijken et al. [49]. By considering a Second Tier Pontoon – STP below a S-S $[4Sc\&4Bp]$ platform, strong changes on the transverse responses due to VIM were observed in Hussain et al. [28]. Recently, changes on the geometry of a S-S $[4Sc\&4Bp]$ were investigated in Xu [67], according to which, large blisters of asymmetric shape and sharp corners were able to break the coherent vortex shedding along the columns.

VIM response measured in full scale is reported in Rijken and Leverette [48], presenting a similar behavior than observed in small-scale tests, although with lower amplitudes. According to the authors, the smaller amplitudes are a consequence of simplifications on the platform geometry, responsible for conservative predictions as also proposed by the measurements of VIM on a truss spar, [31].

A final effect investigated in some VIM model tests of deep draft S-S platforms is related to its coexistence with wave excitation. According to Hong et al. [27], the VIM excitation depends not only on the current velocity, but also on the wave-induced orbital velocity. Probably, the VIM due to the current velocity is disturbed by the wave-induced orbital velocity, particularly near the free surface. As pointed out by the studies on spars, this is a open issue with a series of details deserving further study. Some preliminary results are presented in Stansberg [56], where large irregular waves seem to reduce, in some cases extinguish, the VIM responses.

CONCLUDING REMARKS

In this survey, most of the experimental results available and reported in the open literature on VIM were gathered in order to clearly identify the actual stage of knowledge, trying to highlight the main aspects commonly found in the experimental practices and equally the most striking results observed. Remarkable effort has been done by several research groups and much of the knowledge gathered presents a series of fundamental aspects observed for VIV phenomenon acting on slender bodies, reason for the background based extensively on that subject. Such a strategy comes from that VIM is, in fact, a particular case of the VIV phenomenon, considered under a correct set of parameters.

The next paragraphs summarize the most important remarks for the state-of-art of experimental investigation on VIM, followed by some research prospects.

State-of-art of experimental investigation on VIM

The Reynolds number imposes substantial change on the VIM, but some recent experiments have shown that experiments at subcritical flow are valid, see for instance Roddier et al. [50]. Qualitatively, the small-scale tests bring reliable and conservative prediction for the early stages of platform design. However, it is important to remember that for one case investigated, response amplitudes from small-scale tests overcame in 50% the field measurements, difference that can be assigned to lower Reynolds numbers during the tests, eventual scale effects and/or the characteristic of the excitation in full scale, naturally composed by current flow, wind and waves acting simultaneously.

Towing tank tests is the most common method for studying the VIM of floating platforms. Experiments in an ocean basin make feasible studies considering aspects such as non uniform current profiles of long term, soft mooring systems based on scaled or truncated lines and simultaneous wave excitation. Although substantial effects coming from these aspects have been presented by some works, they still deserve meticulous attention.

The scale factor is one of the most important aspects to be considered for a better similarity in terms: geometric (considering not only the platform geometry but also the appendages); dynamic (taking into account natural periods, mass ratio and reduced velocities); and hydrodynamic similarity (particularly concerning the Froude number in order to avoid free surface effects of unreal nature). In the case o towing tests, blockage effect due to proximity to the wall must also be avoided.

For the VIM dynamic of floating systems is essential to consider not only the sway (transverse motion in relation to the current flow), but also the surge and yaw (respectively, in-line and angular motion in the free surface plane). For simultaneous excitation from waves and current flow, the remaining degrees-of-freedom certainly are important. That is why most of the experimental investigations are based on a floating model restored by an equivalent mooring system. Indeed, the restoring system can be responsible for some differences, mainly in terms of synchronization, but the equivalent mooring system based on horizontal springs is a good solution for VIM tests, as observed by van Dijk et al. [61]. Synchronization for a wider range of reduced velocity has been observed as a consequence of the coupling between in-line and transverse motions.

All the investigations herein reported were conducted for floating units, resulting in mass ratios equal to unity, or even smaller for tension-leg platforms. As observed by Waals et al. [62], the effect of mass ratio on the VIM of offshore units is consistent to the VIV of long cylinders, which creates proper conditions for coupled motions in-line and transverse to the current flow, making of the dynamic similarity in terms of natural periods a important aspect to be properly considered. According to that, trajectories in *8-shape* can be observed for VIM acting on spars and monocolumns, generally related to higher response amplitudes for a wider range of reduced velocity and with no *L-branch* present, such as it happens for cylinder with larger values of aspect ratio. In the case of semi-submersible platforms, the mass ratio equal to unity and the particular geometry seem to be reasons for the similar resonance transverse to the flow current, with larger amplitudes for heading of 45°, but never higher than the column width. Considerable yaw-VIM has been observed for semi-submersible platforms, with larger angular amplitudes for a heading of 0°. However, this angular resonance is not completely understood in terms of its phenomenology, deserving more attention since it can contribute to the fatigue life of risers and mooring lines.

Regardless the platform geometry, VIM responses have been observed even for very low aspect ratios. However, changes of draft has been reported as the most effective action in order to mitigate the phenomenon, although operationally not possible for all the considered geometries. For details about this issue see, for instance, Gonçalves et al. [21] or Magee et al. [37]. As an alternative, suppressors such as strakes has been extensively investigated for application in spars during the last years, but always deeply related to the platform geometry. Even though, three starts of helical strakes 14%D in height seems to be the most efficient geometry for spars, as discussed in Wang et al. [65].

The presence of appendages assembled to the platform hull, such as anodes, mooring chains, fairleads and pipes, is another striking aspect for changes in VIM responses. According to that, a good directional resolution during the tests is decisive for covering all the range of in-line and transverse amplitudes as a function of the reduced velocity, bearing in mind that structures running vertically along the hull, in general, are responsible for better spanwise correlation of vortex shedding and, accordingly, for higher response amplitudes in convenient angles of heading. This information can be useful for installing the platform in a correct heading, *i.e.* where the higher current velocity is coincident to the less sensitive heading. In the case of spar platforms, it is important to remember that holes and cut-outs in the strakes can affect their efficiency.

The simultaneous excitation by current and waves is one of the open issues. Some studies like Finnigan et al. [11], Gonçalves et al. [21] and Hong et al. [27] have showed that simultaneous waves can mitigate the VIM response, however not for any condition of incidence or characteristic amplitude and frequency. A more general investigation is needed, comprising of regular and irregular waves, aligned and oblique to the current flow.

As it is well known, in some cases the VIM response can be strongly modulated in amplitude, generally in the beginning of synchronization range (at lower reduced velocity) and also in its end (at higher reduced velocity), when it exists. In those cases long time histories are necessary for ensuring reliable statistical values. Regardless the aspects related to the applied facility, the improvement of analysis can also be achieved by applying alternative techniques of signal processing, such as the Hilbert-Huang Transform. As presented in Gonçalves et al. [24], the HHT technique can provide better statistics for not so long time histories, especially when they are modulated in amplitude and/or frequency.

Research prospects

As mentioned previously, the coexistence due to VIM and wave-excitation still deserves a better understanding. A comprehensive investigation is needed and requires the consideration of a wide variety of waves, not only for understanding the phenomenology but also for proposing better procedures of how to consider wave-excitation and VIM during the first stages of design, avoiding excessively conservative predictions.

Bearing in mind that experiments with small-scale models in subcritical regimes are the only possible alternative, reliable procedures for the VIM tests are increasingly required, as well as constant improvement of sensoring and analysing them. In fact, numerical simulations via CFD have been improved and the next VIM tests should also keep focus on specific measurements for validation purpose, making of them a complementary tool for investigation of other issues, such as scale effects, VIM in supercritical region, suppressor optimization, among others.

ACKNOWLEDGMENT

Prof. Fujarra is grateful to the Brazilian Navy and Maritime Research Institute Netherlands by all the support provided during his sabbatical year in Wageningen, the Netherlands. During this period, this review could be completed, taking the valuable opportunity of gathering experiences from both the institute and the university. Eng. Rosetti and Eng. Gonçalves would like to acknowledge FAPESP and CAPES, by the funding of their respective PhD programs. The authors from TPN are also thankful for all the support from the Department of Naval Architecture and Ocean Engeneering at University of São Paulo, USP.

REFERENCES

[1] A. Ayoub and K. Karamcheti. An experiment on the flow past a finite circular cylinder at high subcritical and supercritical reynolds numbers. *Journal of Fluid Mechanics*, 118:1–26, 1982. doi: 10.1017/S0022112082000937.

[2] R. D. Blevins and C. S. Coughran. Experimental investigation of Vortex-Induced vibration in one and two dimensions with variable mass, damping, and reynolds number. *Journal of Fluids Engineering*, 131(10):101202–7, 2009. doi: 10.1115/1.3222904.

[3] S. S. Chen and J. A. Jendrzejczyk. Dynamic response of a circular cylinder subjected to liquid cross flow. *Journal of Pressure Vessel Technology*, 101(2):106–112, 1979. doi: 10.1115/1.3454607.

[4] M. Cueva, A. L. C. Fujarra, K. Nishimoto, L. Quadrante, and A. P. Costa. Vortex-induced motion: Model testing of a monocolumn floater. In *Proceedings of the 25th International Conference on Offshore Mechanics and Arctic Engineering. Volume 4: Terry Jones Pipeline Technology; Ocean Space Utilization; CFD and VIV Symposium*, pages 635–642, Hamburg, Germany, 2006. ASME. ISBN 0-7918-4749-7. doi: 10.1115/OMAE2006-92167.

[5] J. M. Dahl, F. S. Hover, and M. S. Triantafyllou. Two-Degree-of-Freedom Vortex-Induced vibrations using a force assisted apparatus. *Journal of Fluids and Structures*, 22(6-7):807–818, 2006. ISSN 0889-9746. doi: 16/j.jfluidstructs.2006.04.019.

[6] J. M. Dahl, F. S. Hover, M. S. Triantafyllou, S. Dong, and G. E. Karniadakis. Resonant vibrations of bluff bodies cause multivortex shedding and high frequency forces. *Physical Review Letters*, 99(14), 2007. doi: 10.1103/PhysRevLett.99.144503.

[7] Z. Ding, S. Balasubramanian, R. Lokken, and T Yung. Lift and damping characteristics of bare and straked cylin-

ders at riser scale reynolds numbers. In *Proceedings of Offshore Technology Conference*. The Offshore Technology Conference, May 2004. ISBN 9781555632519. doi: 10.4043/16341-MS.

[8] D. Farivar. Turbulent uniform flow around cylinders of finite length. *AIAA Journal*, 19:275–281, March 1981.

[9] L. D. Finn, J. V. Maher, and H. Gupta. The cell spar and vortex induced vibrations. In *Proceedings of Offshore Technology Conference*, OTC-15244, Houston, EUA, May 2003.

[10] T. Finnigan and D. Roddier. Spar VIM model tests at supercritical reynolds numbers. In *Proceedings of the 26th International Conference on Offshore Mechanics and Arctic Engineering. Volume 3: Pipeline and Riser Technology; CFD and VIV*, pages 731–740, San Diego, California, USA, 2007. ASME. doi: 10.1115/OMAE2007-29160.

[11] T. Finnigan, M. Irani, and R. van Dijk. Truss spar VIM in waves and currents. In *Proceedings of the 24th International Conference on Offshore Mechanics and Arctic Engineering. Volume 2*, pages 475–482, Halkidiki, Greece, 2005. ASME. doi: 10.1115/OMAE2005-67054.

[12] T. A. Fox and C. J. Apelt. Fluid-Induced loading of cantilevered circular cylinders in a Low-Turbulence uniform flow. part 3: Fluctuating loads with aspect ratios 4 to 25. *Journal of Fluids and Structures*, 7(4):375–386, 1993. ISSN 0889-9746. doi: 06/jfls.1993.1022.

[13] T. A. Fox and G. S. West. Fluid-Induced loading of cantilevered circular cylinders in a Low-Turbulence uniform flow. part 2: Fluctuationg loads on a cantilever of aspect ratio 30. *Journal of Fluids and Structures*, 7(1):15–28, January 1993. ISSN 0889-9746. doi: 06/jfls.1993.1002.

[14] T. A. Fox and G. S. West. Fluid-Induced loading of cantilevered circular cylinders in a Low-Turbulence uniform flow. part 1: Mean loading with aspect ratios in the range 4 to 30. *Journal of Fluids and Structures*, 7(1):1–14, January 1993. ISSN 0889-9746. doi: 06/jfls.1993.1001.

[15] C. M. Freire and J. R. Meneghini. Experimental investigation of VIV on a circular cylinder mounted on an articulated elastic base with two Degrees-of-Freedom. In *Proceedings of the IUTAM Symposium on Bluff Body Wakes and Vortex-Induced Vibrations*, Capry, Italy, June 2010. ISBN BB-VIV6.

[16] A. L. C. Fujarra, C. P. Pesce, F. Flemming, and C. H. K. Williamson. Vortex-Induced vibration of a flexible cantilever. *Journal of Fluids and Structures*, 15(3-4):651–658, 2001. ISSN 0889-9746. doi: 06/jfls.2000.0368.

[17] A. L. C. Fujarra, C. P. Pesce, K. Nishimoto, M. Cueva, and F. Faria. Non-stationary VIM of two Mono-Column oil production platforms. In *Proceedings of the IUTAM Symposium on Bluff Body Wakes and Vortex-Induced Vibrations*, Costa do Sauípe, Brazil, December 2007.

[18] A. L. C. Fujarra, R. T. Gonçalves, F. Faria, M. Cueva, K. Nishimoto, and E. F. N. Siqueira. Mitigation of Vortex-Induced motions in a monocolumn platform. In *Proceedings of the 28th International Conference on Offshore Mechanics and Arctic Engineering. Volume 1: Offshore Technology*, pages 361–374, Honolulu, Hawaii, USA, 2009. ASME. ISBN 978-0-7918-4341-3. doi: 10.1115/OMAE2009-79380.

[19] R. T. Gonçalves, A. L. C. Fujarra, G. F. Rosetti, K. Nishimoto, M. Cueva, and E. F. N. Siqueira. Vortex-Induced motion of a monocolumn platform: New analysis and comparative study. In *Proceedings of the 28th International Conference on Offshore Mechanics and Arctic Engineering. Volume 1: Offshore Technology*, pages 343–360, Honolulu, Hawaii, USA, 2009. ASME. ISBN 978-0-7918-4341-3. doi: 10.1115/OMAE2009-79378.

[20] R. T. Gonçalves, F. T. Matsumoto, E. B. Malta, G. F. Rosetti, A. L. C. Fujarra, and K. Nishimoto. Evolution of the MPSO (monocolumn production, storage and offloading system). *Marine Systems & Ocean Technology*, 5(1):45–53, 2009. ISSN 1679-3962. URL `http://www.sobena.org.br/msot/downloads/MS&OT5V1_3.09.10.pdf`.

[21] R. T. Gonçalves, A. L. C. Fujarra, G. F. Rosetti, and K. Nishimoto. Mitigation of Vortex-Induced motion (VIM) on a monocolumn platform: Forces and movements. *Journal of Offshore Mechanics and Arctic Engineering*, 132: 041102, 2010. ISSN 08927219. doi: 10.1115/1.4001440.

[22] R. T. Gonçalves, C. M. Freire, G. F. Rosetti, G. R. Franzini, A. L. C. Fujarra, and J. R. Meneghini. Experimental comparisons to assure the similarity between VIM (Vortex-Induced motion) and VIV (Vortex-Induced vibration) phenomena. In *Proceedings of the 30th International Conference on Ocean, Offshore and Arctic Engineering. Volume 7: CFD and VIV; Offshore Geotechnics*, pages 11–22, Rotterdam, Holanda, 2011. ASME. ISBN 978-0-7918-4439-7. doi: 10.1115/OMAE2011-49011.

[23] R. T. Gonçalves, G. F. Rosetti, A. L. C. Fujarra, K. Nishimoto, and A. C. Oliveira. Experimental study on Vortex-Induced motions (VIM) of a Large-Volume Semi-Submersible platform. In *Proceedings of the 30th International Conference on Ocean, Offshore and Arctic Engineering. Volume 7: CFD and VIV; Offshore Geotechnics*, pages 1–9, Rotterdam, Holanda, 2011. ASME. ISBN 978-0-7918-4439-7. doi: 10.1115/OMAE2011-49010.

[24] R. T. Gonçalves, G. R. Franzini, G. F. Rosetti, A. L. C. Fujarra, and K. Nishimoto. Analysis methodology for Vortex-Induced motion (VIM) of a monocolumn platform applying the Hilbert-Huang transform method. *Journal of Offshore Mechanics and Arctic Engineering*, 134:011103, 2012. ISSN 08927219. doi: 10.1115/1.4003493.

[25] R. T. Gonçalves, G. F. Rosetti, A. L. C. Fujarra, and K. Nishimoto. Experimental comparative study on Vortex-

Induced motion (VIM) of a monocolumn platform. *Journal of Offshore Mechanics and Arctic Engineering*, 134: 011301, 2012. ISSN 08927219. doi: 10.1115/1.4003494.

[26] R. Govardhan and C. H. K. Williamson. Defining the in Vortex-Induced vibration: Revealing the effect of reynolds number using controlled damping. *Journal of Fluid Mechanics*, 561:147–180, 2006. doi: 10.1017/S0022112006000310.

[27] Y. Hong, Y. Choi, J. Lee, and Y. Kim. Vortex-Induced motion of a Deep-Draft Semi-Submersible in current and waves. In *Proceedings of the 18th International Offshore and Polar Engineering Conference*, Vancouver, British Columbia, Canada, 2008. The International Society of Offshore and Polar Engineers. ISBN 978-1-880653-70-8.

[28] A. Hussain, E. Nah, R. Fu, and A. Gupta. Motion comparison between a conventional deep draft Semi-Submersible and a dry tree Semi-Submersible. In *Proceedings of the 28th International Conference on Offshore Mechanics and Arctic Engineering. Volume 1: Offshore Technology*, pages 785–792, Honolulu, Hawaii, USA, 2009. ASME. ISBN 978-0-7918-4341-3. doi: 10.1115/OMAE2009-80006.

[29] M. Irani and L. Finn. Model testing for vortex induced motions of spar platforms. In *Proceedings of the 23rd International Conference on Offshore Mechanics and Arctic Engineering. Volume 1: Parts A and B*, pages 605–610, Vancouver, British Columbia, Canada, 2004. ASME. doi: 10.1115/OMAE2004-51315.

[30] M. Irani and L. Finn. Improved strake design for vortex induced motions of spar platforms. In *Proceedings of the 24th International Conference on Offshore Mechanics and Arctic Engineering. Volume 1: Parts A and B*, pages 767–773, Halkidiki, Greece, 2005. doi: 10.1115/OMAE2005-67384.

[31] M. Irani, S. Perryman, J. Brewer, and S. McNeill. Vortex induced motions of the horn mountain truss spar. In *Proceedings of the 27th International Conference on Offshore Mechanics and Arctic Engineering. Volume 4: Ocean Engineering; Offshore Renewable Energy*, pages 967–973, Estoril, Portugal, 2008. ASME. doi: 10.1115/OMAE2008-57992.

[32] N. Jauvits and C. H. K. Williamson. The effect of two degrees of freedom on Vortex-Induced vibration at low mass and damping. *Journal of Fluid Mechanics*, 509:23–62, 2004. doi: 10.1017/S0022112004008778.

[33] N. Jauvtis and C. H. K. Williamson. Vortex-Induced vibration of a cylinder with two degrees of freedom. *Journal of Fluids and Structures*, 17(7):1035–1042, June 2003. ISSN 0889-9746. doi: 16/S0889-9746(03)00051-3.

[34] T. Kawamura, M. Hiwada, T. Hibino, I. Mobuchi, and M. Kumada. Flow around a finite circular cylinder on a flat plate : Cylinder height greater than turbulent boundary layer thickness. *Bulletin of the Japan Society of Mechanical Engineers*, 27(232):2142–2151, October 1984.

[35] R. King. Vortex excited structural oscillations of a circular cylinder in steady currents. In *Proceedings of Offshore Technology Conference*, volume 143-149, Dalas, Texas, USA, 1974. doi: 10.4043/1948-MS.

[36] T. Kokkinis, R. E. Sandstrom, H. T. Jones, H. M. Thompson, and W. L. Greiner. Development of a stepped line tensioning solution for mitigating VIM effects in loop eddy currents for the genesis spar. In *Proceedings of the 23rd International Conference on Offshore Mechanics and Arctic Engineering, Volume 1, Parts A and B*, pages 995–1004, Vancouver, British Columbia, Canada, 2004. doi: 10.1115/OMAE2004-51546.

[37] A. Magee, R. Sheikh, K. Y. H. Guan, and J. T. H. Choo. Model tests for VIM of Multi-Column floating platforms. In *Proceedings of the 30th International Conference on Ocean, Offshore and Arctic Engineering. Volume 7: CFD and VIV; Offshore Geotechnics*, OMAE2011-49151, Rotterdam, Holanda, 2011. ASME. ISBN 978-0-7918-4821-0.

[38] T. L. Morse and C. H. K. Williamson. The effect of reynolds number on the critical mass phenomenon in vortex-induced vibration. *Physics of Fluids*, 21:045105, 2009. ISSN 10706631. doi: 10.1063/1.3113522.

[39] T. L. Morse, R. N. Govardhan, and C. H. K. Williamson. The effect of end conditions on the Vortex-Induced vibration of cylinders. *Journal of Fluids and Structures*, 24 (8):1227–1239, November 2008. ISSN 0889-9746. doi: 16/j.jfluidstructs.2008.06.004.

[40] A. Nakamura, A. Okajima, and T. Kosugi. Experiments on Flow-Induced In-Line oscillation of a circular cylinder in a water tunnel (2nd report, influence of the aspect ratio of a cantilevered circular cylinder). *JSME International Journal Series B Fluids and Thermal Engineering*, 44(4):705–711, 2001.

[41] T. Okamoto and M. Yagita. The experimental investigation on the flow past a circular cylinder of finite length placed normal to the plane surface in a uniform stream. *Bulletin of JSME*, 16(95):805–814, 1973. ISSN 00213764.

[42] G. Palau-Salvador, T. Stoesser, J. Fröhlich, M. Kappler, and Wo. Rodi. Large eddy simulations and experiments of flow around Finite-Height cylinders. *Flow, Turbulence and Combustion*, 84:239–275, August 2009. ISSN 1386-6184, 1573-1987. doi: 10.1007/s10494-009-9232-0.

[43] C. W. Park and S. J. Lee. Free end effects on the near wake flow structure behind a finite circular cylinder. *Journal of Wind Engineering and Industrial Aerodynamics*, 88(2-3): 231–246, 2000. ISSN 0167-6105. doi: 16/S0167-6105(00) 00051-9.

[44] C. P. Pesce and A. L. C. Fujarra. Vortex-Induced vibrations and jump phenomenon: Experiments with a clamped flexible cylinder in water. *International Journal of Offshore and Polar Engineering*, 10(1):26–33, March 2000. ISSN 1053-5381.

[45] C. P. Pesce and A. L. C. Fujarra. The 'Super-Upper branch' VIV response of flexible cylinders. In *Proceedings of the IUTAM Symposium on Bluff Body Wakes and Vortex-Induced Vibrations*, Santorini, Greece, June 2005.

[46] K. Raghavan and M. M. Bernitsas. Experimental investigation of reynolds number effect on vortex induced vibration of rigid circular cylinder on elastic supports. *Ocean Engineering*, 38(5-6):719–731, April 2011. ISSN 0029-8018. doi: 10.1016/j.oceaneng.2010.09.003.

[47] O. Rijken and S. Leverette. Experimental study into vortex induced motion response of semi submersibles with square columns. In *Proceedings of the 27th International Conference on Offshore Mechanics and Arctic Engineering. Volume 4: Ocean Engineering; Offshore Renewable Energy*, pages 263–276, Estoril, Portugal, 2008. ASME. ISBN 978-0-7918-4821-0. doi: 10.1115/OMAE2008-57396.

[48] O. Rijken and S. Leverette. Field measurements of vortex induced motions of a deep draft semisubmersible. In *Proceedings of the 28th International Conference on Offshore Mechanics and Arctic Engineering. Volume 6: Materials Technology; C.C. Mei Symposium on Wave Mechanics and Hydrodynamics; Offshore Measurement and Data Interpretation*, pages 739–746, Honolulu, Hawaii, USA, 2009. ASME. ISBN 978-0-7918-4346-8. doi: 10.1115/OMAE2009-79803.

[49] O. Rijken, S. Schuurmans, and S. Leverette. Experimental investigations into the influences of SCRs and appurtenances on deepdraft semisubmersible vortex induced motion response. In *Proceedings of the 30th International Conference on Ocean, Offshore and Arctic Engineering. Volume 6: Ocean Engineering*, OMAE2011-49365, Rotterdam, Holanda, 2011. ASME. ISBN 978-0-7918-4821-0.

[50] D. Roddier, T. Finnigan, and S. Liapis. Influence of the reynolds number on spar vortex induced motions (VIM): multiple scale model test comparisons. In *Proceedings of the 28th International Conference on Offshore Mechanics and Arctic Engineering. Volume 5: Polar and Arctic Sciences and Technology; CFD and VIV*, pages 797–806, Honolulu, Hawaii, USA, 2009. ASME. doi: 10.1115/OMAE2009-79991.

[51] S. C. Roh and S. O. Park. Vortical flow over the free end surface of a finite circular cylinder mounted on a flat plate. *Experiments in Fluids*, 34(1):63–67, 2003. ISSN 0723-4864. doi: 10.1007/s00348-002-0532-6.

[52] T. Rödiger, H. Knauss, U. Gaisbauer, and E. Krämer. Pressure and heat flux measurements on the surface of a Low-Aspect-Ratio circular cylinder mounted on a ground plate. In Cameron Tropea, Suad Jakirlic, Hans-Joachim Heinemann, Rolf Henke, and Heinz Hönlinger, editors, *New Results in Numerical and Experimental Fluid Mechanics VI*, volume 96, pages 121–128. Springer Berlin Heidelberg, Berlin, Heidelberg, 2008. ISBN 978-3-540-74458-0.

[53] H. Sakamoto and M. Arie. Vortex shedding from a rectangular prism and a circular cylinder placed vertically in a turbulent boundary layer. *Journal of Fluid Mechanics*, 126: 147–165, 1983. doi: 10.1017/S0022112083000087.

[54] T. Sarpkaya. Hydrodynamic damping, Flow-Induced oscillations, and biharmonic response. *Journal of Offshore Mechanics and Arctic Engineering*, 117(4):232–238, November 1995. doi: 10.1115/1.2827228.

[55] S. Someya, J. Kuwabara, Y. Li, and K. Okamoto. Experimental investigation of a Flow-Induced oscillating cylinder with two Degrees-of-Freedom. *Nuclear Engineering and Design*, 240(12):4001–4007, 2010. ISSN 0029-5493. doi: 16/j.nucengdes.2010.03.033.

[56] C. T. Stansberg. Current effects on a moored floating platform in a sea state. In *Proceedings of the 27th International Conference on Offshore Mechanics and Arctic Engineering. Volume 4: Ocean Engineering; Offshore Renewable Energy*, pages 433–444, Estoril, Portugal, 2008. ASME. ISBN 978-0-7918-4821-0. doi: 10.1115/OMAE2008-57621.

[57] B. Stappenbelt and F. Lalji. Vortex-induced vibration Super-Upper response branch boundaries. *International Journal of Offshore and Polar Engineering*, 18(2):99–105, June 2008. ISSN 1053-5381.

[58] D. Sumner, J. L. Heseltine, and O. J. P. Dansereau. Wake structure of a finite circular cylinder of small aspect ratio. *Experiments in Fluids*, 37(5):720–730, 2004. ISSN 0723-4864. doi: 10.1007/s00348-004-0862-7.

[59] A. Tahar and L. Finn. Vortex induced motion (VIM) performance of the multi column floater (MCF)_Drilling and production unit. In *Proceedings of the 30th International Conference on Ocean, Offshore and Arctic Engineering. Volume 7: CFD and VIV; Offshore Geotechnics*, OMAE2011-50347, Rotterdam, Holanda, 2011. ASME. ISBN 978-0-7918-4821-0.

[60] R. van Dijk, A. Magee, S. Perryman, and J. Gebara. Model test experience on vortex induced vibrations of truss spars. In *Proceedings of Offshore Technology Conference*, May 2003. doi: 10.4043/15242-MS.

[61] R. R. T. van Dijk, A. Voogt, P. Fourchy, and S. Mirza. The effect of mooring system and sheared currents on vortex induced motions of truss spars. In *Proceedings of the 22nd International Conference on Offshore Mechanics and Arctic Engineering. Volume 1: Offshore Technology; Ocean Space Utilization*, pages 285–292, Cancun, Mexico, 2003. ASME. doi: 10.1115/OMAE2003-37151.

[62] O. J. P. Waals, A. C. Phadke, and S. Bultema. Flow induced motions on multi column floaters. In *Proceedings of the 26th International Conference on Offshore Mechanics and Arctic Engineering. Volume 1: Offshore Technology; Special Symposium on Ocean Measurements and Their Influence on Design*, pages 669–678, San Diego, California, USA, 2007. ASME. ISBN 0-7918-4267-3. doi:

10.1115/OMAE2007-29539.

[63] Y. Wang, J. Yang, Tao Peng, and Xin Li. Model test study on Vortex-Induced motions of a floating cylinder. In *Proceedings of the 28th International Conference on Offshore Mechanics and Arctic Engineering. Volume 5: Polar and Arctic Sciences and Technology; CFD and VIV*, pages 293–301, Honolulu, Hawaii, USA, 2009. ASME. doi: 10.1115/OMAE2009-79134.

[64] Y. Wang, Jian-min Yang, and Hai-ning Lu. Computational fluid dynamics and experimental study of lock-in phenomenon in vortex-induced motions of a cell-truss spar. *Journal of Shanghai Jiaotong University (Science)*, 14(6): 757–762, December 2009. ISSN 1007-1172. doi: 10.1007/s12204-009-0757-0.

[65] Y. Wang, J. Yang, Tao Peng, and Hai-ning Lu. Strake design and VIM-Suppression study of a Cell-Truss spar. In *Proceedings of the 29th International Conference on Ocean, Offshore and Arctic Engineering. Volume 6*, pages 507–513, Shanghai, China, 2010. ASME. doi: 10.1115/OMAE2010-20225.

[66] C. H. K. Williamson and N. Jauvtis. A High-Amplitude 2T mode of Vortex-Induced vibration for a light body in XY motion. *European Journal of Mechanics - B/Fluids*, 23 (1):107–114, January 2004. ISSN 0997-7546. doi: 16/j.euromechflu.2003.09.008.

[67] Qi Xu. A new semisubmersible design for improved heave motion, Vortex-Induced motion and quayside stability. In *Proceedings of the 30th International Conference on Ocean, Offshore and Arctic Engineering. Volume 1: Offshore Technology; Polar and Arctic Sciences and Technology*, OMAE2011-49118, Rotterdam, Holanda, 2011. ASME. ISBN 978-0-7918-4821-0.

[68] T Yung, R. E. Sandstrom, S. Slocum, Z. Ding, and R. Lokken. Advancement of spar VIV prediction. In *Proceedings of Offshore Technology Conference*, May 2004. doi: 10.4043/16343-MS.

TABLE 2: Summary of main aspects and results from the VIM tests on spar platforms.

Ref.	Floating Unit (λ)	Facility Information	Reynolds Number	Aspect Ratio (†)	DOF	(Full scale) Experimental Stiffness	Other Relevant Features	Max. Transv. Response A_y/D (V_r)	Main Results
[9][29]	Cell spar (1 : 47)	Model vertically tested in towing tank and flume	N.A.(‡)	N.A.	6 (floating)	(Taut-leg) Hanging weight system	Different strakes, headings and facilities	0.55 (approx. 6), w/o strakes 0.10 to 0.12 (6 to 7), with strakes	(a) Flume and towing tests are comparable; (b) Strakes deserve attention.
[60]	Truss spar (1 : 67)	Model vertically tested in towing tank	$3.0\cdot10^4$ to $4.0\cdot10^5$	N.A.	6 (floating)	(Semi taut-leg) Horizontal equivalent springs	Different strakes, headings and surface roughness	0.68 (8), w/o strakes 0.10 (8), with strakes	(a) Roughness and heading are quite important; (b) Trajectories in *8-shape*.
[61]	Truss spar (1 : 67)	Model vertically tested in towing tank and offshore basin	$2.5\cdot10^4$ to $1.0\cdot10^5$	N.A.	6 (floating)	(Semi taut-leg) Horizontal springs versus complete mooring	Strakes and current profiles	0.34 (6.5), slab and loop current 0.24 (5.5), hurricane profile Cases w/o strakes	(a) Current profile and mooring system play a role; (b) Horizontal equivalent mooring system is a good alternative.
[36][68]	Classic spar (N.A.)	Double model with a central plate and horizontally towed	N.A.	5.33	1 (only transverse)	(Taut-leg) Actuator and spring system	Appendages and changes on the mechanical damping	0.25 to 0.60 (5 to 7), with strakes	A complete description about the solution adopted for the VIM on Genesis spar.
[11]	Truss spar (1 : 40)	Model vertically tested in towing tank and offshore basin	$1.1\cdot10^5$	>1.87	6 (floating)	(N.A.) Mooring system based on linear springs and a drag compensation line	Uniform and Step current concomitant with irregular waves (in-line, transverse e oblique)	0.23 (7), w/o waves 0.07 (7), with in-line waves 0.20 (7), with transv. waves 0.19 (8), with oblique waves	(a) Comparable results from offshore basin and towing tank; (b) In-line waves reduces VIM; (c) Transverse and oblique waves promote small changes.
[31]	Truss spar (1 : 1)	Field measurements	Approx. $3.3\cdot10^7$	>1.66	6 (floating)	(Semi taut-leg)	Intrinsic shear current profile, turbulence, waves and wind	0.26 (approx. 6)	(a) Field measurements are well below design values; (b) Each spar is unique in terms of model testing
[63]	Hard tank of a truss spar (1 : 100)	Model fixed, in forced-motion and free to oscillate in ocean basin	$1.8\cdot10^4$ to $4.2\cdot10^4$	2.04	6 (floating)	(Semi taut-leg) Two mooring systems based on 3 or 4 linear springs	Different strakes and headings, also qualitative flow visualization	0.80 (approx. 6) or even higher	(a) No accurate data from the flow visualization; (b) C_L from forced-motion are higher than from fixed cylinder; (c) 14% strakes are more efficient; (d) Headings change the correlation between in-line and transverse motions (*8-shape*)
[64][65]	Cell-truss spar (1 : 100)	Model vertically tested in ocean basin	$7.4\cdot10^3$ to $4.4\cdot10^4$	>2.04(⸸)	6 (floating)	(Semi taut-leg) Truncated mooring system	Different strakes, and current profiles	0.75 (approx. 7), w/o strakes 0.25 (approx. 11), with strakes	(a) W/o strakes, the synchronization seems no longer be maintained for V_r greater than 10; (b) the suppression structure based on 4 start of inserted strakes with 14%D was the most efficient.
[10][50]	Hard tank of a truss spar (1 : 142.8) (1 : 65) (1 : 22.3)	Straked model vertically tested in 3 different towing tanks	$4.1\cdot10^4$ to $1.7\cdot10^6$ (in 3 ranges	1.70	6 (floating)	Spring catenary shape	Headings and appendages	0.80 to 0.90 (7.5 to 10)	(a) Testing at subcritical Re is acceptable and slightly conservative; (b) Little differences between subcritical and supercritical results for $Vr \leqslant 7$.

(†) It was assumed L/D, where L and D are draft and hydrodynamic diameter of the hard tank, respectively.

(‡) The information is not available.

(⸸) It was assumed L/D, where L is the draft and D is the sum of central and two outer cell diameters.

TABLE 3: Summary of main aspects and results from the VIM tests on monocolumn platforms.

Ref.	Floating Unit (λ)	Facility Information	Reynolds Number	Aspect Ratio (†)	DOF	(Full scale) Experimental Stiffness	Other Relevant Features	Max. Transv. Response A_y/D (V_r)	Main Results
[4]	MonoGoM (‡) (1 : 200)	Model vertically tested in towing tank	$2.0 \cdot 10^4$ to $1.0 \cdot 10^5$	0.39	6 (floating)	(Semi taut-leg) Horizontal equivalent springs	Roughness on the model surface, headings, appendages and spoiler plates for VIM suppression	1.38 (13)	(a) Sufficient roughness was able to emulate a supercritical regime; (b) Higher response amplitudes for $V_r > 8$, as a consequence of motion in *8-shape* at the free surface; (c) Once started, it was not observed an end for the synchronization region; (d) Spoiler plates were efficient in mitigating the VIM responses.
[17]	Sevan Piranema (⸸) (1 : 200)	Model vertically tested in towing tank	$4.0 \cdot 10^4$ to $2.0 \cdot 10^5$	0.22	6 (floating)	(Semi taut-leg) Horizontal equivalent springs	Roughness on the model surface, headings, appendages and different drafts	0.63 (11)	(a) Lower response amplitudes as a result of the lower aspect ratios ; (b) The Hilbert-Huang Transform (HHT) is presented as an innovative technique for signal processing coming from VIM tests, that assures better statistics.
[18][21]	MonoBR (⸷) (1 : 200)	Model vertically tested in towing tank	$5.0 \cdot 10^4$ to $2.0 \cdot 10^5$	0.39	6 (floating)	(Semi taut-leg) Horizontal equivalent springs	Headings, drafts, concomitant regular waves; external damping and spoiler plates	0.95 (14.5)	(a) Headings are decisive for VIM of monocolumns; (b) The regular wave can mitigate VIM, particularly when its period is close to the natural period of heave; (c) Decrease of draft is the most decisive effect to mitigate VIM on monocolumns; (d) Higher damping coming from riser system can change substantially the VIM responses.
[19][25]	MonoGoM (1 : 90) (1 : 200)	Model vertically tested in towing tank	$2.0 \cdot 10^4$ to $1.0 \cdot 10^6$ (in 4 ranges)	0.39	6 (floating)	(Semi taut-leg) Horizontal equivalent springs in 4 arrangements	Roughness on the model surface, headings, appendages, mooring arrangements and different facilities with distinct scales	1.38 (approx. 13), for model scaled by $\lambda = 200$ and supported by 4 mooring lines 0.88 (approx. 13), for model scaled by $\lambda = 90$ and supported by 3 mooring lines	(a) Roughness on the model is not only capable of representing the supercritical drag region, but also increases the repeatability of the tests; (b) The coupled motions in *8-shape* are responsible for sustaining the high amplitudes for a larger range of velocities; (c) Tests for $V_r > 12$ are necessary to identify potential synchronization region and better behaved motions of high amplitude; (d) Mooring system and/or scale seem to play a role on the amplitude response.

(†) It was assumed L/D, where L and D are draft and main hydrodynamic diameter of the floating body.

(‡) Monocolumn designed for operating at Gulf of Mexico.

(⸸) Monocolumn operating at the northeast of Brazil.

(⸷) Monocolumn designed for operating at Campos Basin, Brazil.

TABLE 4(a): Summary of main aspects and results from the VIM tests on semi-submersible and tension leg platforms.

Ref.	Floating Unit (λ)	Facility Information	Reynolds Number	$(H/L)^{(\dagger)}$ (S/L) (H/P)	DOF	(Full scale) Experimental Stiffness	Other Relevant Features	Transverse Response at 45° $A_y/L^{(\natural)}$ (V_r)	Main Results
[62]	3 Floaters [4Sc&4Bp] and 1 Floater [4Sc&2Bp] (1 : 70)	Models tested in towing tank	$6.0\cdot10^3$ to $6.0\cdot10^4$	(1.75)(0.87) (4.14) (2.33)(1.16)	3 (surge, sway and yaw)	(Semi taut-leg and tensioned tendons) Air bearings to provide vertical pretension and 2 horizontal springs	Headings, drafts and mass ratios. Also, different geometries: deep draft S-S; deep draft TLP; S-S (4 pontoons) and S-S (2 pontoons)	0.45 (7) for deep draft S-S 0.48 (7) for deep draft TLP 0.08 (15) for S-S 4 pontoons 0.54 (6) for S-S 2 pontoons	(a) The effect of m^* for VIM on floater is consistent with VIV on long cylinders; (b) the largest motions were observed for 45° of heading; (c) Large yaw motions at higher V_r seem to be related to a galloping phenomenon.
[47]	Deep draft S-S with [4Sc&4Bp] (1 : 50)	Model tested in towing tank	$1.0\cdot10^4$ to $1.0\cdot10^5$	(2.18) (3.75) (4.83)	6 (floating)	(N.A.)$^{(\ddagger)}$ 4 Horizontal equivalent springs	Headings, appendages, concomitant small sea state and external damping	0.66 (6.5) w/o small sea state and external damping	(a) For smaller angles of heading, range over which synchronization occurs is larger than that for 45° , but with smaller A_y/L; (b) VIM increases the drag load; (c) Relatively small sea states don't influence the VIM response; (d) Increase of damping up to 10% did not change the VIM response.
[27]	Deep draft S-S with [4Sc&4Bp] (1 : 60)	Model tested in ocean basin	$4.3\cdot10^4$ to $1.1\cdot10^5$	(N.A.) (4.19) (N.A.)	6 (floating)	(Semi taut-leg) 4 truncated lines in catenary geometry	Headings and concomitant waves	0.31 (6.7) w/o waves	(a) S_t similar to that from circular cylinders; (b) VIM also depends on the wave-induced particle velocity.
[28]	Deep draft S-S with [4Sc&4Bp] (1 : 69.5)	Models tested in towing tank	$5.6\cdot10^3$ to $9.3\cdot10^4$	(N.A.) (N.A.) (N.A.)	6 (floating)	(Semi taut-leg) 12 truncated lines coupled to mechanical actuators by cables and linear springs	Headings and effects due to a Second Tier Pontoon (STP)	0.50 (21.5) w/o STP 0.64 (17.5) with STP	(a) VIM responses in sway and yaw are most important; (b) Higher yaw responses are related to currents from ahead, while pronounced sway responses are observed at oblique currents; (c) The STP changes the VIM behavior.
[56]	S-S with [4Sc&4Bp] (1 : 55)	Model tested in ocean basin	N.A.	(N.A.) (4.08) (N.A.)	6 (floating)	(Catenary lines) Two configurations: horizontal springs and distinct 12-leg catenary system	Mooring effect and concomitant irregular waves	N.A.	(a) VIM depends on natural frequencies; (b) Large waves seem to reduce or extinguish VIM; (c) Responses due to intrinsic current fluctuations are smaller than wave-induced responses and wave-current interactions.
[48]	Deep draft S-S with [4Sc&4Bp] (1 : 1)	Field measurements	N.A.	(2.18) (3.75) (4.83)	6 (floating)	(Semi taut-leg)	Intrinsic shear current profile, turbulence, waves and wind	Approx. 0.20 (N.A.). Current profile was not measured. Mean current vector was inferred from the offsets	(a) VIM was observed in full scale, with a similar behavior than that in the small-scale tests; (b) Responses from tests are higher than field measurements; (c) Tests derive conservative predictions, probably due to the simplified mooring system, without influence of risers.

$^{(\dagger)}$ In this work, it was assumed as aspect ratio.

$^{(\ddagger)}$ The information is not available.

$^{(\natural)}$ Nominal response, defined as $\sqrt{2}std\{y(t)\}/L$, where L is the face dimension of the column.

[4Sc&4Bp] Means four square columns and four box shaped pontoons. [4Sc&2Bp] Means four square columns and two box shaped pontoons.

TABLE 4(b): Continuing the summary of main aspects and results from the VIM tests on semi-submersible and tension leg platforms.

Ref.	Floating Unit (λ)	Facility Information	Reynolds Number	$(H/L)^{(\dagger)}$ (S/L) (H/P)	DOF	(Full scale) Experimental Stiffness	Other Relevant Features	Transverse Response at 45° $A_y/L^{(\natural)}$ (V_r)	Main Results
[23]	Deep draft S-S with [$4Sc\&4Bp$] (1 : 100)	Model tested in towing tank	$6.0 \cdot 10^3$ to $9.0 \cdot 10^4$	(1.14)(0.23) (3.76) (1.98)(0.40)	6 (floating)	(Semi taut-leg) 4 Horizontal equivalent springs	Headings and appendages	0.40 (7 to 8)	(a) Transverse synchronization occurs always for $4 \leqslant V_r \leqslant 14$, with some differences depending on the considered heading; (b) Yaw-VIM perfectly identified with $\alpha_{max} = 4.5°$; (c) No trajectories in *8-shape* were identified for tests.
[37]	TLP with [$4Sc\&4Bp$] (1 : 70)	Model tested in towing tank. Also fixed, close to a S-S	$1.0 \cdot 10^4$ to $8.0 \cdot 10^4$	(1.00)(1.50) (N.A.) (N.A.)	6 (floating like a S-S, $m^* = 1$)	(Tension-leg) 4 Horizontal equivalent springs	Headings and drafts	0.45 (8)	(a) Higher transverse amplitudes occur for $8 \leqslant V_r \leqslant 10$ and for 45° heading; (b) Higher yaw motions occur for 0° heading; (c) Draft changes affect more the response for 45° than for 0° heading.
[49]	Deep draft S-S with [$4Sc\&4Bp$] (1 : 48) (1 : 56.5)	Models tested in two different towing tanks.	$9.0 \cdot 10^4$ to $8.8 \cdot 10^5$	(1.72)(0.44) (4.04)(2.20) (3.04)(0.79)	6 (floating) and 3 (surge, sway and yaw)	(N.A.) 4 Horizontal equivalent springs and for some tests 2 extra springs emulating the stiffness from SCR's	Headings, appendages and extra stiffness from SCR's	Approx. 0.65 (6.8)	(a) The extra stiffness coming from the SCR's don't change the VIM behavior; (b) Detailed appendages only play a role when located on the vertical faces of the columns and above pontoon level.
[59]	Deep draft S-S with [$4x4Tc\&4Bp$] (1 : 55.9)	Model tested in towing tank	up to $5.0 \cdot 10^5$	(1.74) (3.20) (4.00)	6 (floating)	(N.A.) 4 Taut lines and 1 extra line emulating the stiffness from risers	Headings and appendages	0.47 (approx. 6)	(a) Higher transverse amplitudes occur for 45° heading; (b) Measurements of drag force were performed and drag coefficients appear to be in constant relationship with response amplitudes.
[67]	2 Deep draft S-S with [$4Sc\&4Bp$]: conventional and other with blisters and tapered pontoons (N.A)	Models tested in towing tank	(N.A.)	(1.55)(1.45) (3.65) (3.10)(2.42)	6 (floating)	N.A.	Headings, appendages and differences between both geometries	0.58 (7 to 8) for the conventional S-S 0.20 (10) for the S-S with blisters and tapered pontoons	(a) The large blisters of asymmetric shape and sharp corners are able to break vortex shedding coherence along the column length, reducing VIM responses.

($\dagger$) In this work, it was assumed as aspect ratio.

($\ddagger$) The information is not available.

($\natural$) Nominal response, defined as $\sqrt{2}std\{y(t)\}/L$, where L is the face dimension of the column.

[$4Sc\&4Bp$] Means four square columns and four box shaped pontoons. [$4Sc\&2Bp$] Means four square columns and two box shaped pontoons. [$4x4Tc\&4Bp$] Means four by four tubular columns and four box shaped pontoons.